SINET: Ethiop. J. Sci., 45(2): 143–164, 2022 ISSN: 0379–2897 (PRINT)
 eISSN: 2520–7997

Date received: May 06, 2022; Date revised: August 15, 2022; Date accepted: August 18, 2022
DOI: https://dx.doi.org/10.4314/sinet.v45i2.3

Petrology and geochemistry of bimodal volcanic rocks of Southern Lake Hayk area, northwestern Ethiopian plateau: implication for their petrogenesis

Getie Berlie [1,*], Dereje Ayalew [2] and Mohammed Assen [1,2]

[1] Department of earth science, Samara University, PO Box 132, Samara, Ethiopia. E-email;getieberlie12@gmail.com
[2] School of Earth Sciences, Addis Ababa University, PO Box 1176, Addis Ababa, Ethiopia

ABSTRACT: This study presents and integrates field, petrological, and whole-rock geochemical (major and trace elements) data of the volcanic rocks from the Lake Hayk area to understand their petrogenesis. The study area's major lithological components include lower and upper basalt, rhyolitic lava, rhyolitic tuff, rhyolitic ignimbrite, and unwelded tuff. Petrographic analysis suggests that felsic rocks are dominated by quartz and well-developed sanidine (K-feldspar) phenocrysts with glassy groundmass, whereas mafic volcanic products are characterized by aphyric to porphyritic textures with the olivine and plagioclase dominant phenocryst. The area constitutes bimodal composition of flood basaltic to rhyolitic rock with scarce intermediate composition. Basalts have low Rb/Nb = 0.5-0.58, La/Nb = 0.88-1.06 and high TiO_2 = 2.08-3.04, basaltic andecite have higher Rb/Nb =2.7, La/Nb = 1.81 and low TiO_2= 1.96 and rhyolite Rb/Nb = 0.97-1.69, La/Nb = 0.51-1.08 and lower TiO_2 = 0.41-0.71.The positive Ba and negative K anomalies testify amphibole mantle source. The basalts are characterized by low CaO/Al_2O_3 ratios (0.71–0.97) and relatively less fractionated and flat HREE patterns with (TbN/YbN = 1.75-2.33) chondritic values. This suggests a mantle source mostly containing spinel rather than garnet. Rhyolites are characterized by a steep negative correlation in bivariate plots of MgO, Fe_2O_3, TiO, and CaO against SiO_2 and positive anomaly of Ta with slight Nb trough. This suggests that Fractional Crystallization is the major process for the genesis of rhyolitic rocks, rather than crustal contribution, partial melting, and assimilation, producing rhyolitic rocks.

Key words/phrases: crustal contamination, fractional crystallization, major and trace elements, mantle source, petrogenetic process

INTRODUCTION

Continental flood volcanism (CFV) is associated with rupturing of the Earth's lithosphere. As continental breakup progresses into developed rifting, the geochemical characteristics of the lavas typically change to those of oceanic lavas (ocean island basalts, OIBs; and mid-oceanic ridge basalts, MORBs), implying that upper mantle elements are more involved (Pik et al., 1999). Although continental flood basalt (CFB) provinces are typically associated with deep-origin hot mantle plumes, higher mantle and crustal sources play a significant role in their formation (Richards et al., 1989). Nevertheless, the dating of relationships between rifting leading to ocean-floor formation and continental flood basalt (CFB) formation are complex and can vary in space and time (Courtillot et al., 1999; Hawkesworth et al., 1999). Several petrogenetic models have been presented to explain the formation of silicic volcanic rocks in mafic igneous provinces. Rhyolites and associated silicic volcanic rocks (60 - 81 wt% SiO_2) are generated by a combination of processes. (i) Assimilation and fractional crystallization (AFC) of mafic magma with significant crustal contribution or melting of continental crust (Dereje Ayalew et al., 2002; Dereje Ayalew and Gezahegne Yirgu, 2003, Haldera *et al.*, 2020), and (ii) Parental mafic magma fractional crystallization with minimal crustal contamination (Dereje Ayalew et al., 2002; Haldera et al., 2020). According to Haldera et al. (2020), rhyolites derived by significant fractional crystallization have a modest to non-existent Nb-Ta anomaly, the occurrence of clinopyroxene phenocrysts, and steeply negative slopes in bivariate major oxides plots against SiO_2. Further, Dereje Ayalew et al. (2002) have documented that the plateau rhyolites are geographically correlated with the basalts, low- TiO_2 and high- TiO_2 rhyolites occurring in association with low- TiO_2 and high- TiO_2 flood basalts. Although the area is largely basaltic, the Oligocene volcanic products of the northern Ethiopian plateau show a significantly bimodal distribution of basalts and rhyolites (Dereje Ayalew and Gezahegne Yirgu, 2003). As noted for other continental flood basalt provinces, the coincidence of basalt and rhyolite provinciality suggests that the rhyolites were derived either by fractional crystallization of the associated basalt magma types or by partial

*Author to whom correspondence should be addressed.

melting of underplated basic igneous rocks (Dereje Ayalew et al., 2002). However, intermediate composition (53–66 wt. % SiO_2) rocks are lacking in continental flood basalt provinces, and strong silica gap of volcanic successions (Mohr and Zanettin, 1988; Pik et al., 1998). The Lake Hayk region is in South Wollo, Amhara Regional State, Ethiopia(Fig.1).The study area is predominately dominated by aphyric, porphyritic, and vesicular basalt, and a wide variety of silicic rocks are found in these areas that include dominantly rhyolite (strongly welded), ignimbrite, obsidian, less welded rhyolitic, and volcanic ash deposits. These lithological units are mafic and felsic in composition, however, the mafic composition of rock units covers the majority of the area. The major lithological units located in the study area are exposed due to different activities like stream cut, fault scarps, road cut, hill side, and query site are the most common exposure site of rock outcrops. The research area is characterized by a variety of landforms, ranging from flat areas (plains) to steep slopes (chain of hills). Elevation ranges from 1700 to 2850 (a.m.s.l) with a mean elevation of 2155 m above sea level. Most of the geochemical studies of Ethiopian volcanic Provence were done at regional scale, with only a few comprehensive investigations on isolated plateau parts. The present study is conducted on volcanic rocks that belong to the flood basalt sequence to assess their petrogenesis and source rock characterization.

Regional geological setting

East Africa has at least 720,000 km^3 of Cenozoic magmatic products, mostly basaltic lavas and secondary rhyolites/tuffs (Rooney, 2017). Ethiopia's flood basalts cover 600,000 km^2 and are made up of basaltic and felsic volcanic rock strata (or traps) (fig.1). The thickness of this volcanic pile varies greatly, although it can reach two kilometers in some areas. According to Mohr &Zanettin (1988) and Mohr (1983b), the total volume of volcanic and shallow intrusive rocks is approximately 350,000 km^3. Kieffer et al. (2004) documented that the relative volumes of flood and shield volcanics in the Northern Ethiopia plateau can be approximated as follows; Flood basalts cover a total area of about 240,000km^2 and the total volume of flood basalts is 180,000km^3 if the average thickness is 0.75km. Shields now cover around 20% of the plateau's surface, although they may have covered one-third before erosion. The Ethiopian volcanic plateau, according to Kieffer et al. (2004) is not a thick, monotonous, rapidly erupted pile of undeformed, flat-lying tholeiitic basalts. Instead, it is composed of a variety of volcanic centers with varying magmatic characteristics and ages. The tectonic context and a decline in magma flux, rather than a change in magma composition, are most likely to contribute for the shift of volcanic style.

The plateau's lavas formed from a vast region of mantle upwelling that was distinctive in temperature and content (Kieffer et al., 2004; Rooney, 2017). The majority of them are tholeiitic to transitional in composition (Mohr, 1983a; Mohr & Zanettin, 1988; Pik et al., 1998). Felsic lavas and pyroclastic rocks of rhyolitic or less typically, trachytic compositions interlayer with flood basalts, especially at high stratigraphic levels (Dereje Ayalew et al., 1999).

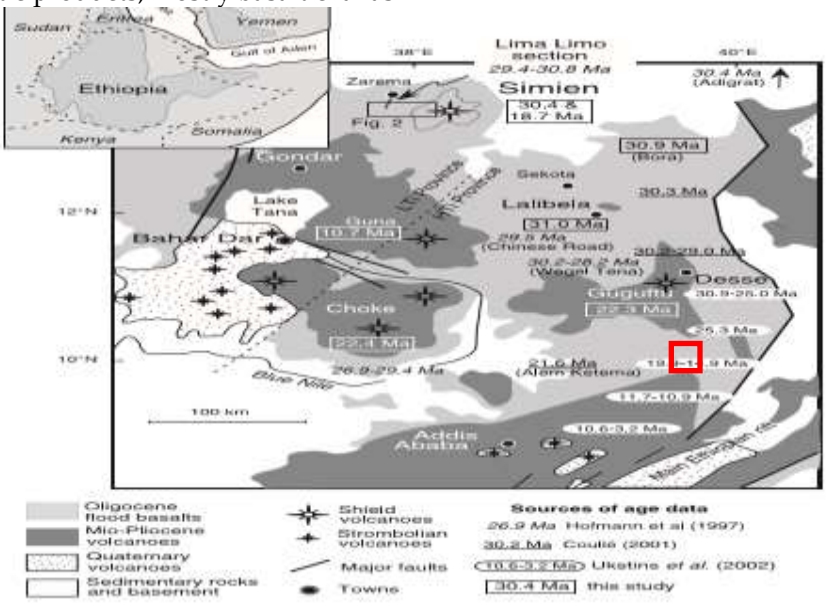

Figure 1. Flood volcanism on the Ethiopian plateau in the North Flood volcanism, as well as the dates and locations of the major shield volcanoes, are displayed on a map of the northern Ethiopian plateau (modified from Pik et al., 1999; Zanettin, 1992), Using age data from this study as well as Hofmann et al. (1997), Coulie (2001), Ukstins et al., (2002), and Coulie et al., (2003). According to Pik et al,(1999)the dashed line denotes the border between the LT and HT provinces.

According to conventional classification, the Ethiopia's Tertiary volcanic sequence is divided into four groups based on their ages and stratigraphic position. From bottom/old to top/young, these are known as the Ashange, Aiba, Alaje, and Termaber Formations (Mohr, 1983). Based on their geochemical makeup the flood basalts are further divided into three groups: low Ti basalts (LT), high Ti1 basalts (HT1), and high Ti2 basalts (HT2) (Pik et al, 1998 & 1999). According to Dereje Ayalew (2019) the ages of marginal rhyolites may be classified into four categories: Oligocene trap rhyolites (28.5–30.8 Ma, on average 30 Ma), early Miocene rhyolites (17.4–23.5 Ma, on average 20 Ma), Rhyolites from the late Miocene to Pliocene epochs (between 8 and 4 Ma), as well as Quaternary rhyolites.

Sampling and analytical technique

15 representative rock samples were prepared for petrographic characterization and 10 samples were prepared for major and trace element l analysis. To remove the weathered part from the surface of the rock samples, the selected pieces were broken by hammer into the desired sizes. Following drying, the samples were crushed to 70% of less than 2 mm, riffled to separate the bulk samples, and the splits were ground to 93.3 % of less than 75 microns. The powdered samples were submitted to Australian Laboratory Science (ALS), to determine the concentration of major and trace elements. Inductively Coupled Plasma Atomic Emission Spectrometry (ICP-AES) was used to examine major elements, whereas Inductively Coupled Plasma Mass Spectrometry was used to examine trace elements (ICP-MS). Besides, multi-element four acid digestions 81(ME-4ACD81) were used for base metal determinations such as Cr, Co, Ni, and V. In addition, loss on ignition (LOI) at 1000 ˚C is determined by an instrument WST-SEQ. The precision of all measured samples is within the confidence level, with major elements like MgO and Na2O having precisions of 0.1 to 0.2 % and 0.01 %, respectively, especially in comparison to SiO2, Al2O3, Fe2O3, CaO, and K2O.

Other than transitional metals, the precision of the most of trace elements, including REE, is better than 0.6 %.The precision is better than 2% for transitional metals including Co, Cu, Zn, Sc, and Ni.

RESULTS

Geology and petrography

The study area which constitutes Oligocene volcanic rock (flood basalts 31 Ma to shield volcano 25Ma) (Hoffmann et al., 1997; Kieffer et al., 2004; Dereje Ayalew et al., 2019). The mappable rock units that cover the study area are lower basalt, upper basalt, rhyolite lava, and rhyolitic tuff (Fig.3A). The study area constitutes different volcanic rock units with different texture, mineral assemblages which shows their origin, evolution, and nature of magma generation. Volcanic rock in the study area are flood basalt (70-190m) In the form of sheet, low viscosity magma covering the bottom part or overline by rhyolitic lava(10 – 230 m) and shield volcanoes composed of successive layers of lava flows and pyroclasts and its thickness is (360 m). Flood volcano in the study area includes porphyritic basalt and aphyric basalt and welded rhyolite overlies flood basalt and at the top there is shield volcano constitutes intercalation of strongly welded rhyolite, less welded rhyolite, ignimbrite, amygdaloidal basalt, shied basalt, and glassy rhyolite (fig.4). The flood volcano separated with shield volcano by reddish colored paleosol (near to 30 cm thickness). Farther volcanic rocks of the study area can be classified into mafic and felsic based on their color and visible mineralogical composition. The mappable rock units that are found in the study area are lower basalt, upper basalt, rhyolitic lava, rhyolitic tuff, and friable tuff. Furthermore, the study area is associated with geological structures such as joints and faults. Petrographically analyzed samples (fig.5) were selected based on their stratigraphic position and lithologic variation. The porphyritic basalts observed in the study area constitute phenocrysts of clinopyroxene, plagioclase, and olivine with a groundmass of microcrystals of plagioclase, pyroxene, and opaque mineral (Fe-Ti oxide) with porphyritic and seriate textures majority of the samples. Rhyolite rock units, in addition to basalt rock samples, are characterized by a vitrophyric to porphyritic texture with phenocrysts of quartz and sanidine, and groundmass of volcanic glass, as well as rock fragments (fig.5). Petrographically, Olivine-Clinopyroxene Phyric Basalt rock unit is characterized by its highly porphyritic texture with phenocrysts of dominantly by olivine and secondly by clinopyroxene and embedded in groundmass very fine plagioclase and opaque mineral (Fe-Ti oxide). With a modal percentage of 70.51 – 76.8% phenocrysts of 36.88 - 41.5% olivine and 33.63 - 35.3% clinopyroxene and 15.3 – 23.2 % of groundmass of 8.6 - 9.5% microcrystalline plagioclase and 6.7 - 14.7% opaque mineral. The mineral grain shows a seriated texture because of the presence of a wide range of grain size variations from very fine plagioclase and clinopyroxene grain to coarse-grained olivine and clinopyroxene. Furthermore, olivine and clinopyroxene phenocrysts have a subhedral to euhedral shape, with irregular cracks and modest iddingsite alteration along the fissures in the olivine grain. Aphyric basaltic rocks found in the

study area which is aphyric in hand sample and petrographically microcrystalline in thin section when analyzed under petrographic microscope. These rocks have a dark gray color in hand samples, and crystals that are undetectable to the naked eye have a glassy appearance. In thin section, they contain few phenocrysts with some indistinguishable mineralogy in groundmass. The rock consists of <7% phenocrysts of euhedral to subhedral plagioclase and clinopyroxene. This unit is dominantly composed of microcrystal of plagioclase and with groundmass of pyroxenes and opaque mineral. Petrographically, Plagioclase Phyric Basalt rock unit is characterized by its highly porphyritic texture with phenocrysts of plagioclase and embedded in the groundmass of microcrystals of plagioclase, clinopyroxene, and opaque mineral (Fe-Ti oxide). The modal composition of this rock unit is dominated by phenocrysts of plagioclases the mineralogical modal percentage is ~75.5% and ~24.3% groundmass, which are composed of 71.5 - 81.3% plagioclase phenocryst with a groundmass of5 - 18.7% clinopyroxene and 9.7 - 20% opaque mineral. Plagioclase, clinopyroxene, and opaque mineral microcrystalline textures account for the majority of the groundmass. In addition, plagioclase phenocrysts show subhedral to euhedral shape and occur as elongated penetrative twinning nature. Petrographically analyzed rhyolite rock samples such as T1S6, T4S5, T2S5, and T3S4. These rhyolitic rock samples show vitrophyric, Porphyritic, glassy, and banding texture flow. Phenocrysts are alkali feldspar (sanidine) and quartz minerals embedded in the groundmass of mainly volcanic glass and very few opaque minerals. Sample T3S4 shows that flow banding microstructure and felsic texture with phenocrysts (10%) and groundmass (90%). Sample T1S6, T2S5, and T3S4 show similar petrographic characteristics. The rhyolite sample that petrographically analyzed shows porphyritic texture with 29.5-65.2% phenocrystsand, 34.87-0.44% groundmass /volcanic glass. Compositionally, 18.5 - 27.5% sanidine, 3 - 35.7% quartz, 1% plagioclase, 4.2-8.9% opaque, and 30.8-62.3% a groundmass of microlithic sanidine, quartz, volcanic glass, and opaque. Once more, sample a similar petrographic characteristic. Rhyolitic Ignimbrites: One sample T3S1 from the pyroclastic flow deposit is classified as welded tuff/ignimbrite. It has up to 21.25% nepheline, 3.75% clinopyroxene, perlitic crack 16%, 10.24% rock fragments, and 54.4% volcanic glass. Crystals are euhedral sanidine and anhedral clinopyroxene and quartz and also contain skeleton-like glass shards.

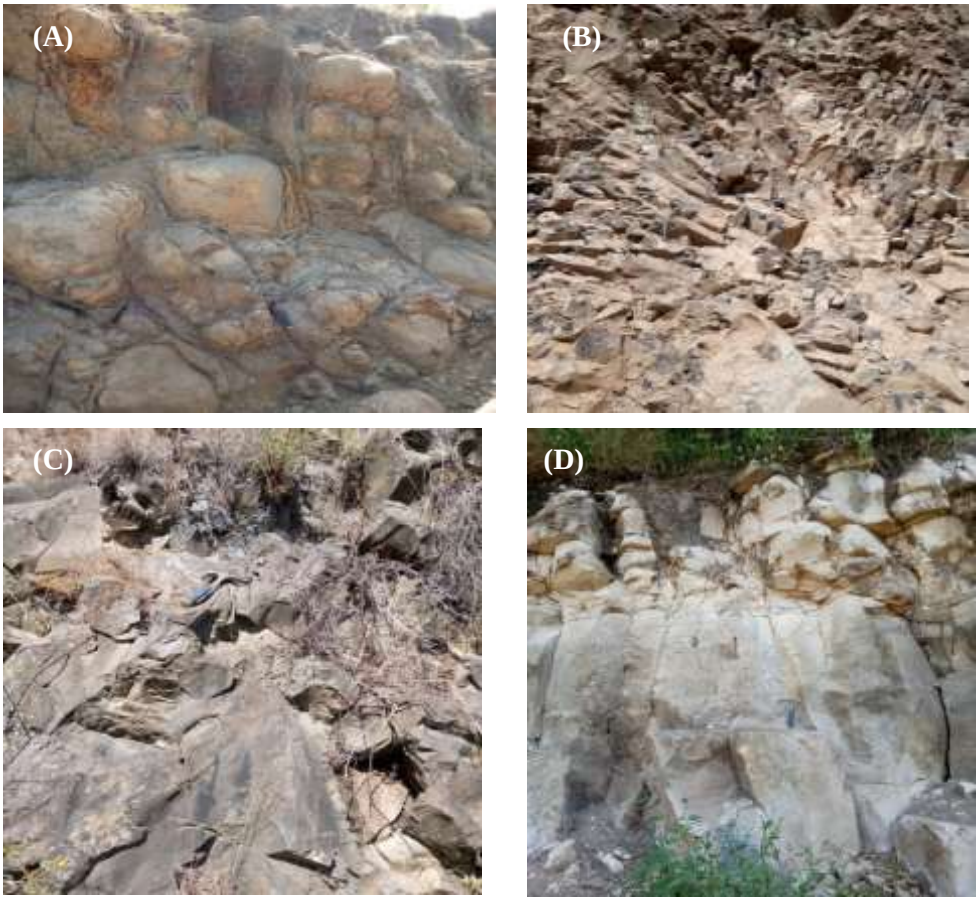

Figure 2. Field photographs of Lake Hayk area (A) Lobe structure solid cores. (B) Complex columnar jointing observed at the top of rhyolite sequence. (C) Aphyric basalt (D) Rhyolite rock unit with vesicles at top part. Note hammer for scale.

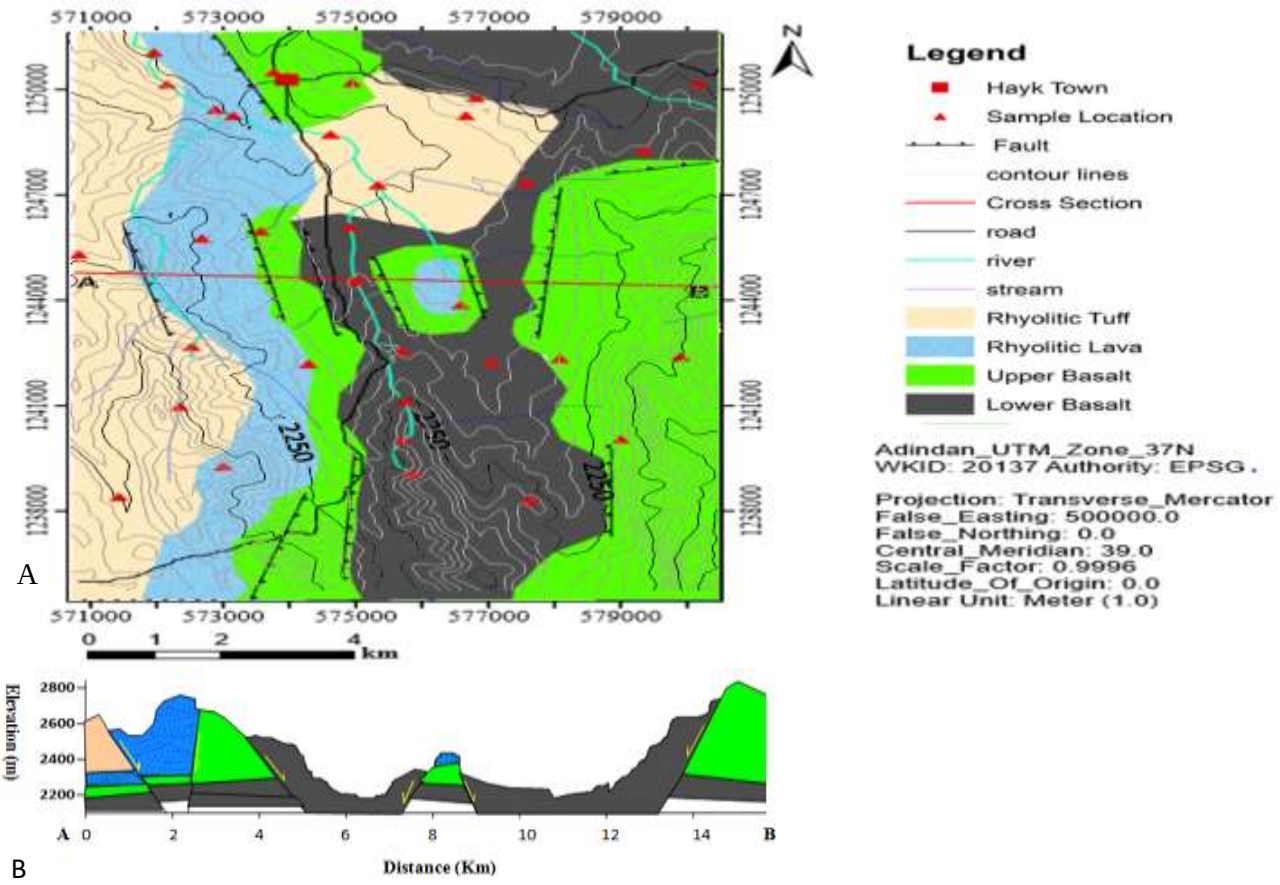

Figure.3. (A), Geological map of the study area and (B), schematic geological cross section (A to B) of Lake Hayk area.

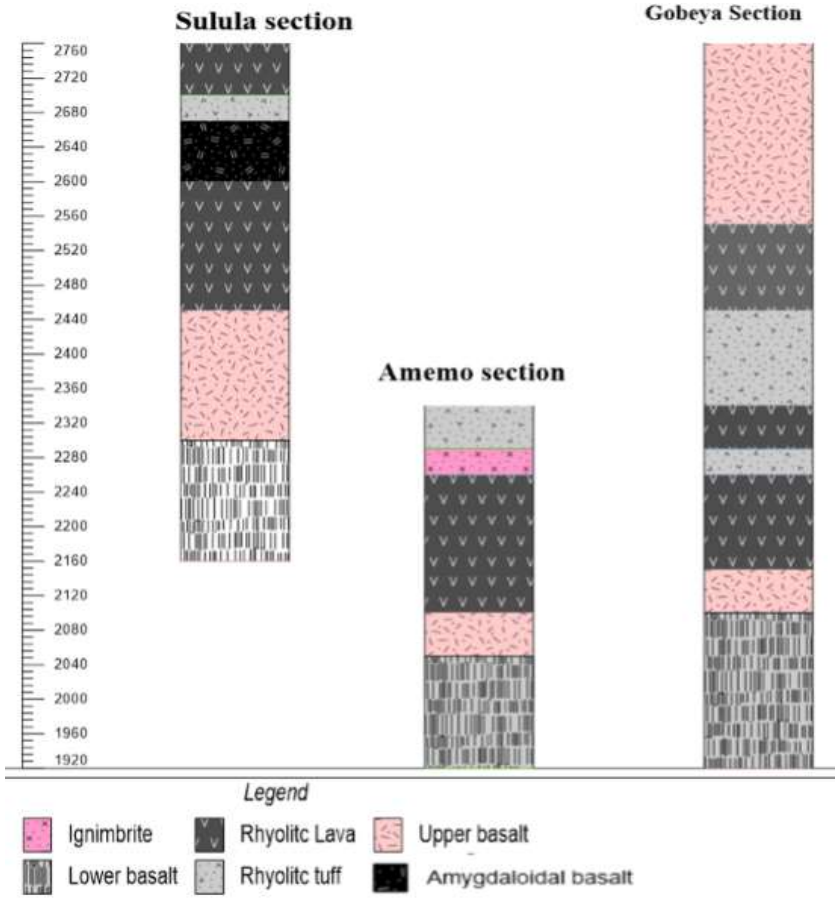

Figure 4. Volcanic stratigraphic section of the study are.

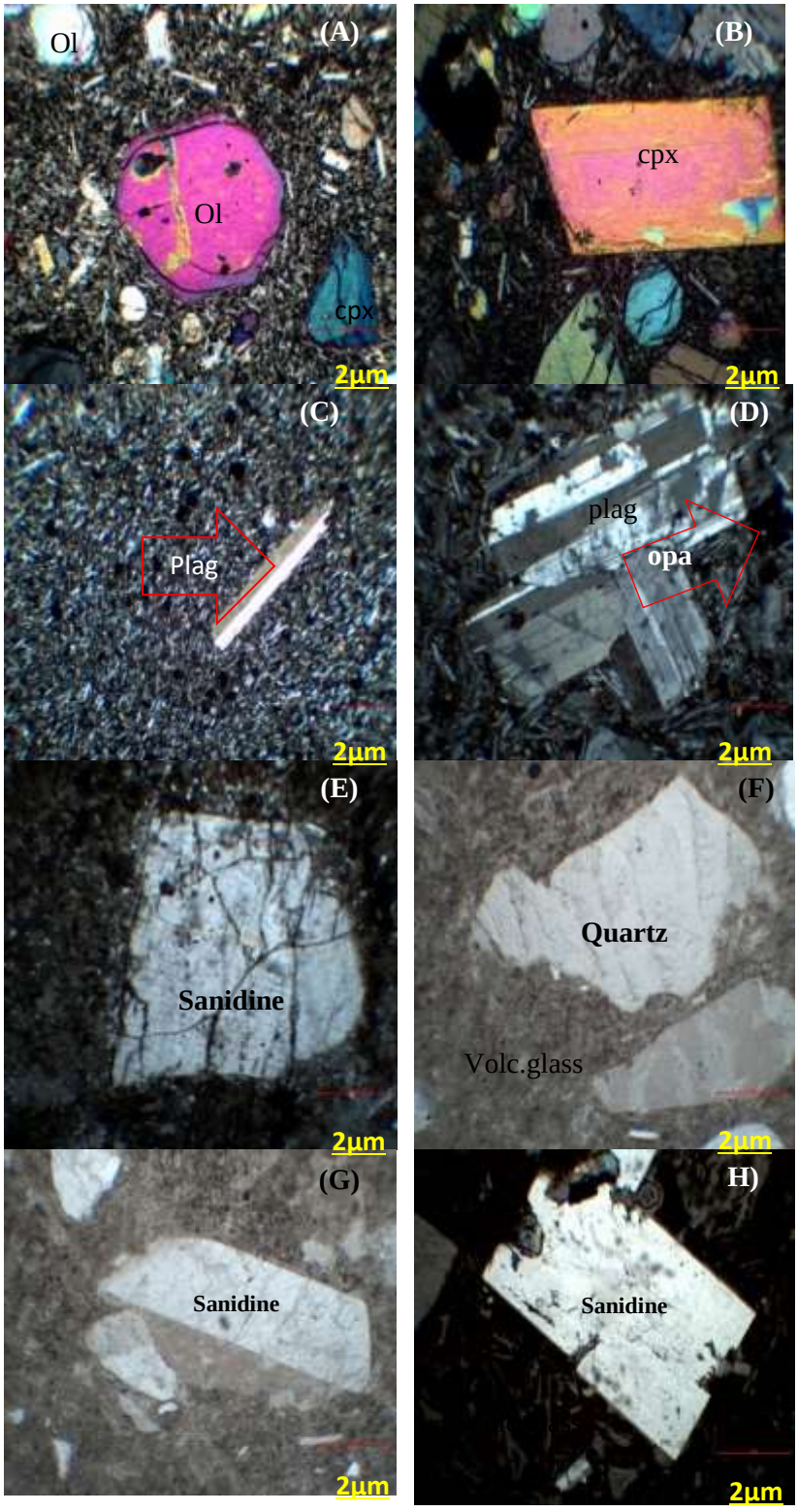

Figure.5. Photomicrographs of representative textures and modal mineralogy of basalts and rhyolite (A),Subhedral to euhedral-shaped phenocrysts of megacryst olivine(ol)and embedded in a groundmass are dominantly fine-grained plagioclase laths and fine-grained clinopyroxene (CPX) with striate texture.(B), Euhedral shaped phenocrysts of clinopyroxene with fine to coarse-grained laths and olivine embedded by fine-grained plagioclase groundmass.it shows a seriate texture. (C), Intersertal texture of aphyric basalt with elongated plagioclase embedded in microcrystals of plagioclase and opaque mineral. A sample is from on the upper flood basalt (2207 masl). (D), phenocryst of plagioclase (plag) embedded in opaque mineral (Fe-Ti oxides), clinopyroxene, and fine plagioclase groundmass, it has Glomerophyric texture, subhedral shape with oscillatory zoning. (E), a euhedral phenocryst of alkali feldspar (sanidine) embedded in volcanic glass (Volc.glass) and microlithic sanidine and quartz.(F), subhedral quartz megacryst phenocryst with a groundmass of volcanic glass and opaque minerals (G),euhedral sanidine and anhedral quartz phenocrysts embedded in volcanic glass and microlithic sanidine and quartz (H), Rectangularlly developed euhedral shape sanidine, subhedral clinopyroxene and rock fragment with groundmass of volcanic glass.

Table 1. Major element wt. % and trace element ppm data of Lake Hayk volcanic rocks.

Sample	T1S1	T2S3	T7S5	T7S1	T3S2	T3S6	T1S3	T3S4	T5S2	T2S1EA
SiO_2	45.5	48.4	48.5	55.9	63.7	66.7	69.7	71.3	72.3	77
TiO_2	3.04	2.08	2.37	1.96	1.04	1.08	0.41	0.54	0.71	0.47
Al_2O_3	11.9	15.25	14.25	15.15	15.55	13	14.65	11.95	13.65	10.5
Fe_2O_3	13.1	11.9	12.25	11.15	5.29	5.36	2.99	3.49	2.72	2.17
FeOt	11.79	10.71	11.03	10	4.76	4.83	2.691	3.2	2.25	1.95
MnO	0.21	0.18	0.18	0.17	0.18	0.24	0.06	0.08	0.07	0.07
MgO	9.16	6.16	7.56	3.94	1.35	0.92	0.16	0.25	0.25	0.08
CaO	11.85	11.75	9.93	7.61	3.1	1	0.22	0.28	1.04	0.1
Na_2O	2.31	2.66	2.62	3.34	5.22	4.69	3.76	4.4	4.57	2.66
K_2O	0.88	0.45	0.81	1.88	2.58	4.48	4.09	5.02	4.21	5.53
P_2O_5	0.53	0.28	0.32	0.29	0.26	0.26	0.03	0.09	0.1	0.01
LOI	1.49	1.07	1.5	0.44	1.57	1.55	3.07	1.04	0.68	1.01
Total	100.1	100.27	100.4	101.9	99.98	99.39	99.19	98.48	100.39	99.61
#Mg	58.31	50.87	55.24	41.41	33.8	25.56	9.6	12.53	6.87	6.08
Sc	33	32	29	25	8	8	4	5	6	6
V	337	301	287	268	23	41	10	18	11	14
Cr	490	110	410	30	<10	10	<10	<10	<10	<10
Co	53	44	46	34	3	4	1	1	2	1
Ni	135	51	97	15	<1	13	4	2	3	1
Cu	159	96	40	31	1	6	1	1	1	<1
Zn	113	103	108	109	117	161	122	163	108	176
Ga	20.5	20.6	19.7	20.2	24.5	31	29.9	34.4	25.1	28.8
Rb	20.6	8.5	10.9	40.2	67.8	102	111.5	123	124.5	136
Sr	546	471	405	342	455	222	21.5	35.1	151	8.6
Y	25.6	23.7	25.3	29.9	39.2	56.8	95.7	90.6	57.2	18.8
Zr	247	146	161	215	452	849	893	1010	623	1190
Yb	1.89	2.26	2.42	2.91	3.76	5.01	10.2	8.1	5.99	3.33
Nb	35.4	17	19.7	14.9	51.6	100.5	114.5	120	73.7	117
Cs	0.33	0.11	0.07	0.22	1.26	0.66	0.81	0.76	1.01	0.61
Ba	256	176.5	260	501	738	774	430	343	698	105
La	31.1	18.1	19.5	27	52.7	88.2	106	104	79.6	59.8
Ce	66.4	39.3	42.1	54.9	110.5	190.5	103.5	219	149.5	92
Pr	9	5.5	5.61	6.98	13.8	24.3	28.4	28.7	19.25	10.1
Nd	37.8	24.4	24.6	30.5	57.4	99.5	110	116.5	74.3	39.9
Sm	8.1	5.8	5.63	6.56	11.15	20.5	21.8	24.9	14.25	7.57
Eu	2.33	1.88	1.9	1.88	3.09	5.28	3.12	4.82	2.66	1.44
Gd	6.82	5.81	5.81	6.48	10	16.45	18.7	21.1	12	5.46
Tb	0.94	0.88	0.88	0.97	1.42	2.31	2.99	3.27	1.9	0.76
Dy	5.45	5.13	4.98	5.52	7.51	12.1	17.8	17.9	10.6	3.89
Ho	0.91	0.92	0.93	1.09	1.39	2.19	3.36	3.28	2.02	0.77
Er	2.36	2.6	2.6	3.11	3.97	5.85	10.15	9.1	5.93	2.28
Tm	0.31	0.35	0.35	0.43	0.58	0.81	1.52	1.29	0.85	0.42
Yb	1.89	2.26	2.42	2.91	3.76	5.01	10.2	8.1	5.99	3.33
Lu	0.3	0.29	0.34	0.42	0.56	0.69	1.45	1.16	0.86	0.57
Hf	5.8	4	4	5.7	11.2	20.7	22.1	24.7	15.7	28.1
Ta	2.1	0.8	0.9	0.9	3.3	6.1	6.8	7.4	4.4	8.1
Pb	<2	<2	2	7	10	5	15	14	13	15
Th	2.9	1.5	2.1	2.93	7.2	11.65	17	16.05	14.3	16.9
U	0.86	0.43	0.43	0.48	2.39	4.04	3.4	5.23	3.38	1.18
Eu/Eu*	0.98	1.00	1.01	0.89	0.90	0.88	0.48	0.65	0.63	0.62

Major elements

Diagrams with their descriptions and interpretation of major elements are based on the recalculated volatile free basis results. The analytical results for both major and trace elements are presented in Table.1.Diagrams with their descriptions and interpretation of major elements are based on the recalculated volatile free basis. Based on SiO_2 versus $Na_2O + K_2O$ (wt %) (TAS) Lake Hayk volcanic rocks are classed as basalt, basaltic andesite, trachydacite, and (following Le Bas et al, 1986).Most of the samples fall on the boundary line of transitional to sub alkaline/tholeiitic field indicating that mostly transitional to sub-alkaline/tholeiitic affinity. Major elements against silica SiO_2 are illustrated below in Harker variation diagrams (Fig.8).The examined samples loss of ignition (LOI) ranges from 0.44 to 1.57 %, showing that the samples are fresh; whereas one sample (T1S3) has a LOI of 3.07 %,(table.1) Therefore, only one sample could be used to determine how post-emplacement alteration affected elemental mobility.

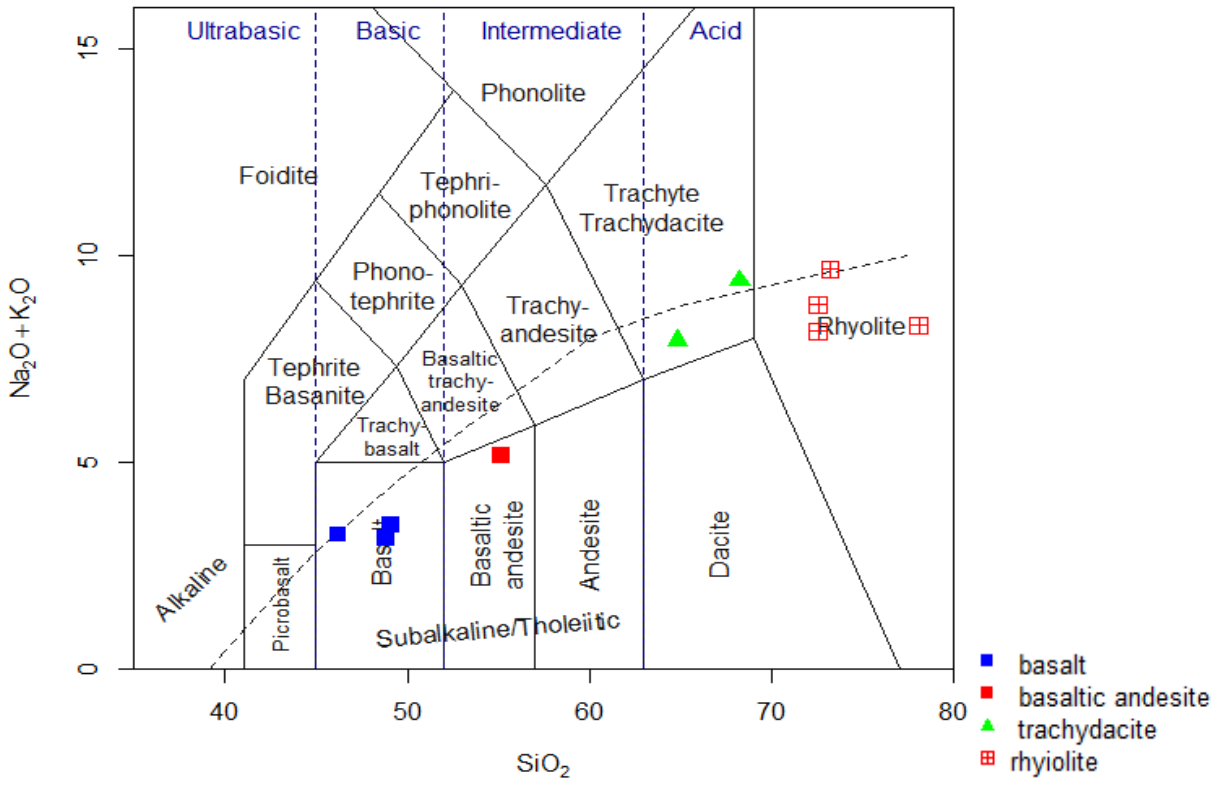

Figure 6. TAS **classification diagram of Lake Hayk volcanics.**

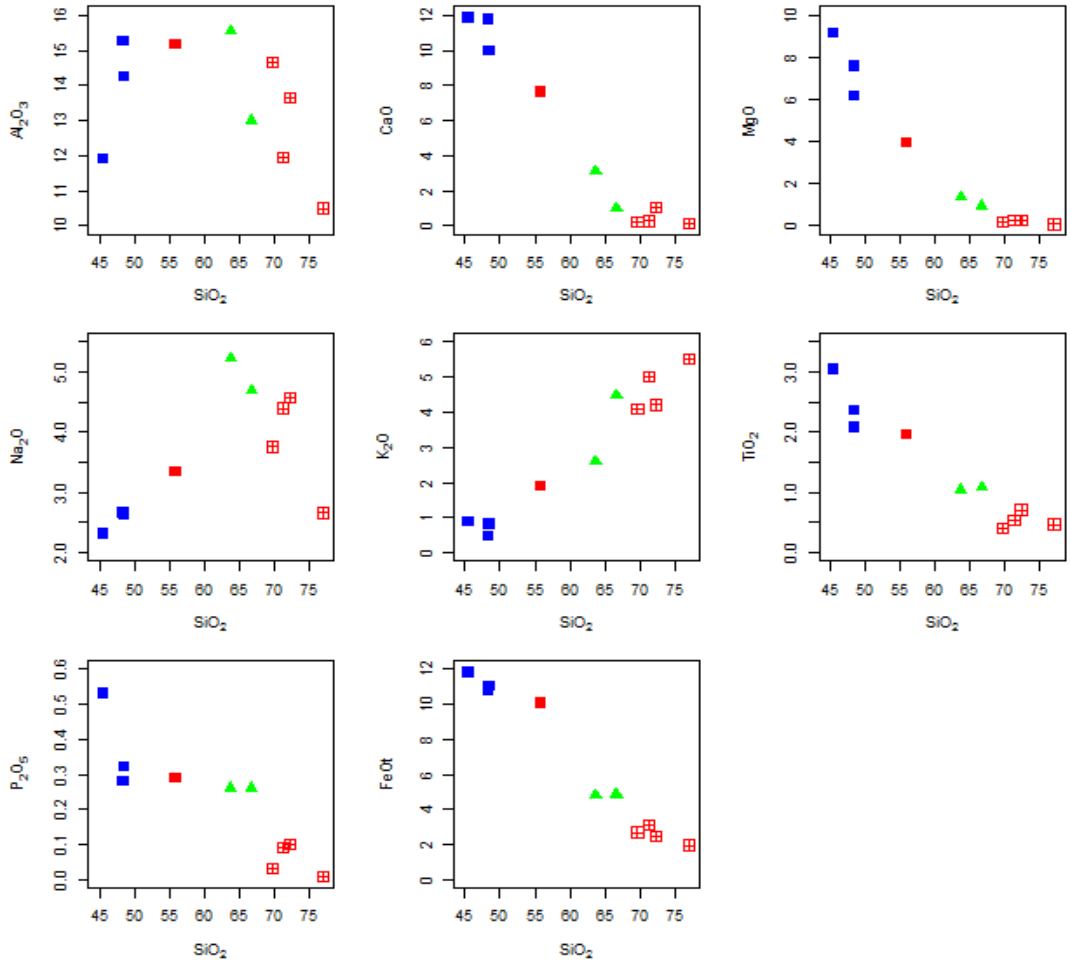

Figure 7. Harker variation diagrams of major element against SiO_2. Symbols are the same as in Fig.6.

Trace elements

The most common incompatible trace elements are large ion Lithophile (LIL)/ (Cs, K (not shown), Rb, Eu, Ba, and Sr) and high field strength (HFS) elements (e.g. Zr, Hf, Ti, Nb, Th, U, Ce, Ta, and Pb). In Fig. 9 diagrams of incompatible trace element (ppm) variation as a function of SiO_2 demonstrate a clear trend of magma evolution. K and Rb have significant positive trend as a function of SiO_2, but Sr has a strong negative correlation trend. The variation diagrams of HFSE (U, Hf, Y (which is not shown in the diagrams below) Th, La, Zr, Nb,) against SiO_2 plotted below (Fig.9) show positive correlations variably with well-defined evolution trend. Plots of Th, U, La, Zr, Hf, and Nb as a function of SiO_2 show a negative correlation up to ~50 wt% of SiO_2 then gradually increase and positive correlation with SiO_2 (50-70wt%), but narrow variation for those incompatible elements as silica increase, and La and U negatively correlated with SiO_2 after ~70. wt%; whereas, Pb against SiO_2 show positive correlation and Y gradually increase up to ~65wt% and in between ~65wt% - ~70 wt% sharply increase and positively correlated; whereas after > 70wt% inflected and negatively correlated. All compatible elements (such as Ni, V, Cr and Co) in the variation diagrams show negative correlation plotted as a function of SiO_2 wt %. A compatible element shows almost similar characteristics to corresponding major elements having negative correlation e.g. Fe_2O_3, MgO, CaO, and TiO_2.

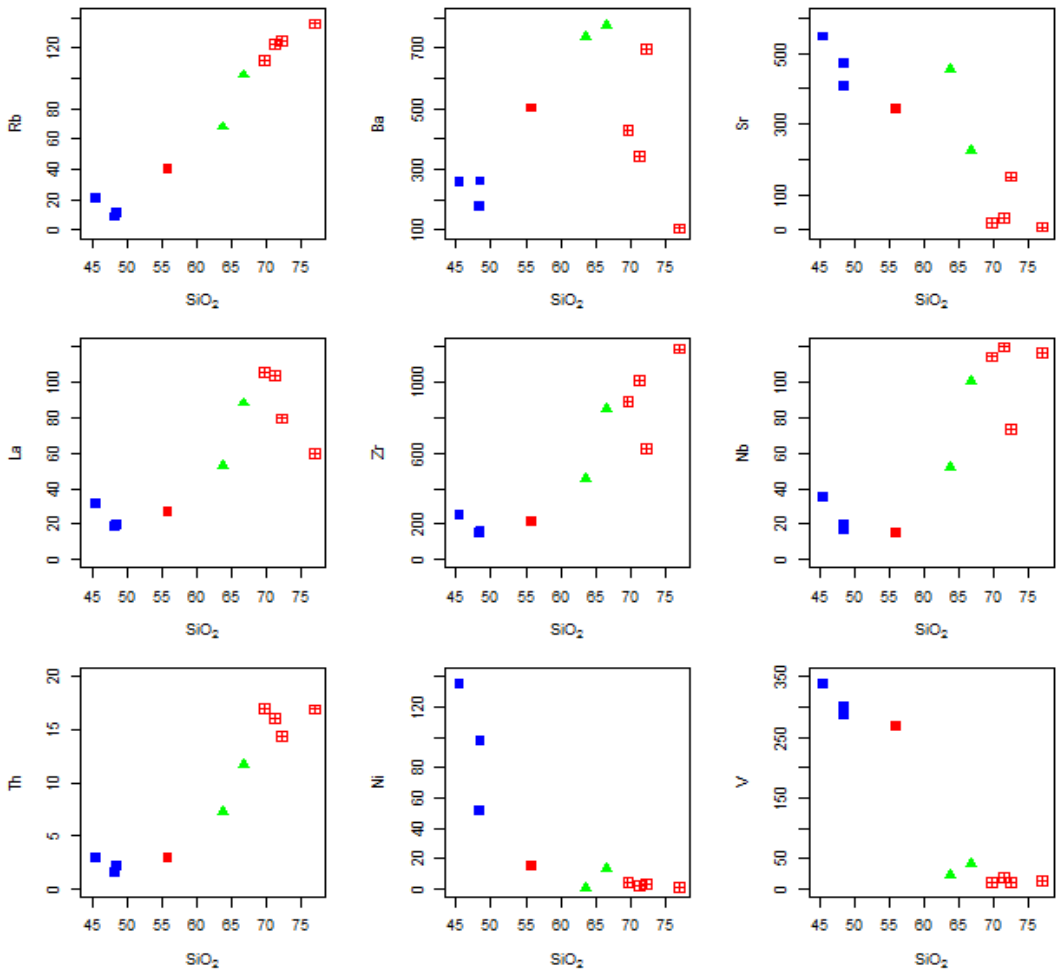

Figure 8. Harker variation diagrams of trace elements against SiO_2. Symbols are the same as in Fig.6.

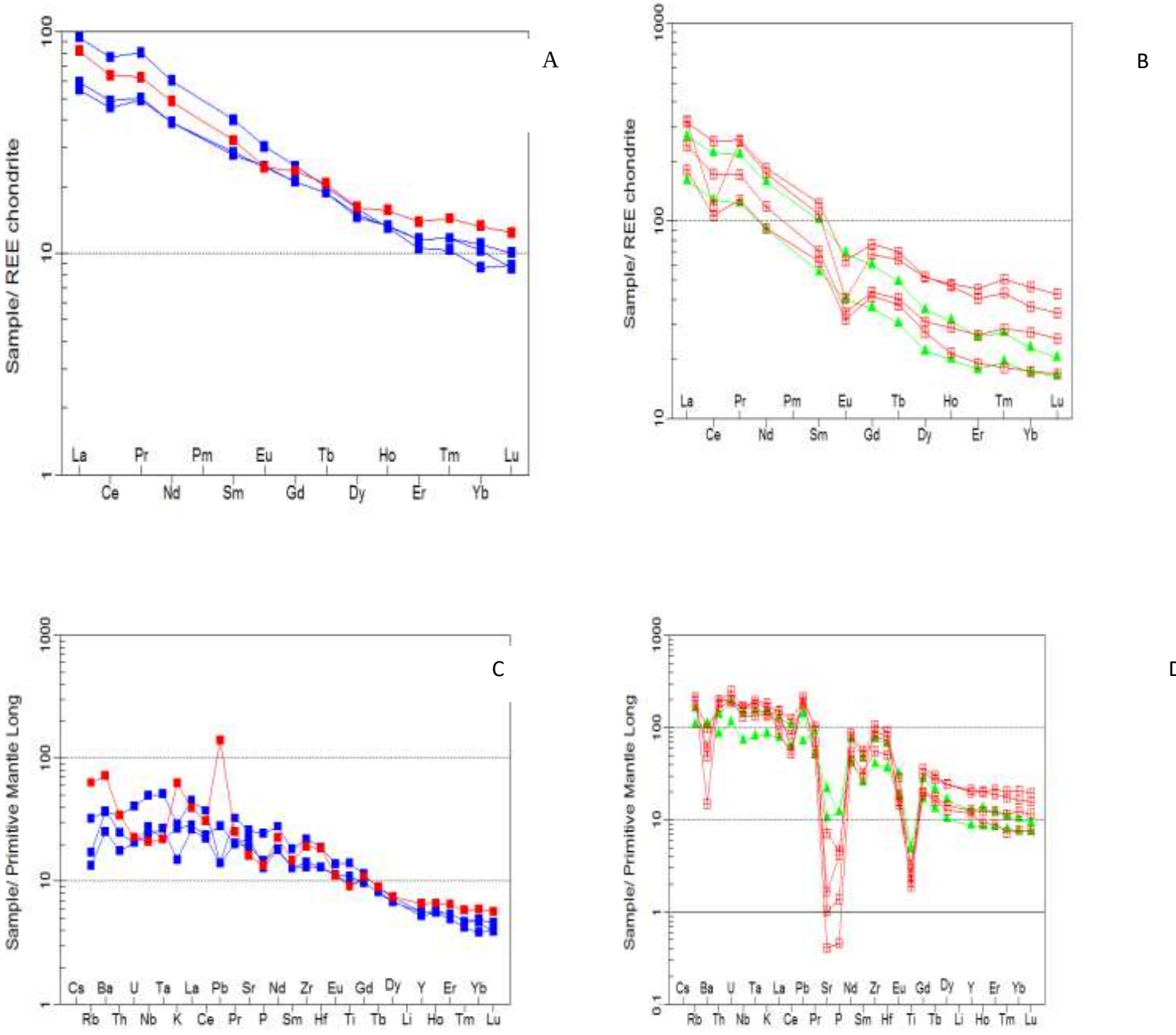

Figure.9. A,B are Chondrite normalized REE pattern of basaltic to basaltic andesite and trachydacite to rhyolite resepectivelly of Lake Hayk analyzed samples. The normalization values are from Nakamura,(1974). C, D are Primitive mantle normalized multi-element variation diagram (Sun and McDonough, 1989) of basaltic to basaltic andesite and trachydacite to rhyolite resepectivelly of Lake Hayk analyzed samples. Symbols are the same as in (Fig.6).

The Spider diagram of mafic to felsic rocks is plotted in fig.9 A and B. All the basaltic and rhyolitic samples are parallel and trachydacite to rhyolitic samples show sub-parallel patterns. The REE chondrite normalized diagram for samples shows a likely pattern of OIB basalt which is enriched in LREE and depleted in HREE. The normalized value of Eu/Eu* is 0.98 -1.01 for mafic/ basalt, 0.88-0.89 for basaltic andesite to trachydacite, and 0.48-0.65 for acidic/rhyolitic samples. Basaltic rock show slight negative anomaly of Ce and also, There is one rhyolite sample (T1S3) showing highly depleted Ce than the other and also which has higher LOI (3.07).

DISCUSSION

Geochemically associated Oligocene basaltic erupted at 31 Ma and rhyolitic volcanic rocks ranges in age from 28.5–30.8 Ma around Lake Hayk are belonging to a bimodal suite. Geochemical data, such as major and trace elements, are used to study the petrogenetic evolution of Lake Hayk flood basalt (31 Ma) and differentiation of rhyolite volcanic rocks. In this section discusses the petrogenetic progression of basalt to rhyolite volcanic rocks in detail. The examined basalt samples from Lake Hayk are characterized by wide ranges in compatible trace element contents. Ni (51-135 ppm), Cr (110-490 ppm, MgO (6.16 - 9.16) wt%. However, primary magma in equilibrium with a typical upper mantle mineral assemblage is characterized by their higher compatible trace element contents such as Ni (>400–500 ppm), Cr (>1000 ppm), and MgO content (10–15 wt. %) (Frey et al., 1978; Hess, 1992). Hence, the values of compatible element and MgO in the studied basalts are lower than primary magma suggesting that they do not represent primary magmas and have undergone fractionation of olivine and clinopyroxene. In addition to this the concentrations of basalt, basaltic andesite, trachydacite, and rhyolitic volcanic rocks contains Sr (405-546 ppm), (345ppm), (222 - 455ppm), and (8.6-151 ppm) and for V (287-337 ppm), (268 ppm) (23-41) and (10-18 ppm) respectively for each rock unit. These suggest there is less fractionation of plagioclase and Fe–Ti oxides in basalt than basaltic andesite to rhyolite (Dereje Ayalew and Gibson, 2009).

Fractional crystallization

The mineralogical modal composition of analyzed samples shows a wide range of textural and mineralogical compositions. Porphyritic basalt, aphyric basalt, rhyolite, and ignimbrite are the volcanic rocks that are petrographically examined which are stratigraphically from bottom to top. Different mineral phases of phenocrysts, microphenocrysts, and groundmass levels with different modal percentages are presented in the rock units. The phenocrysts of porphyritic basalt are olivine and clinopyroxene with a groundmass of microcrystals of plagioclase and opaque mineral (Fe-Ti oxide) which is the bottom part of the study area overlain by aphyric basalt which is composed of plagioclase, some pyroxene with a groundmass of opaque mineral and this aphyric basalt which is overlain by strongly welded rhyolite rocks unit which constitutes of alkali feldspar (sanidine), quartz with a groundmass of volcanic glass and very less opaque mineral it intercalated with less welded rhyolite, ignimbrite(composed of nepheline, rock fragments, and volcanic glass) and with aphyric basalt in some part of the study area(mostly western part). The textural arrangements, the zoning in plagioclase, alteration effects in olivine, clinopyroxene and plagioclase, the euhedral-Subhedral-anhedral shape of phenocryst phase with variations in size, are very common in petrographic analyzed flood basalt rocks and euhedral sanidine, nepheline, and subhedral to anhedral quartz in silicic rocks. Furthermore, the analyzed volcanic rock show differences in crystal shape which implying the order of magma crystallization as euhedral-Subhedral which is the first crystallized minerals, and anhedral crystals crystallized at the last. Plagioclase is normally zoned with a compositional change from the high-temperature mineral phase at the core (Ca-plagioclase) and to low-temperature composition mineral at its rim (Na-plagioclase) and it shows complex zoning, polysynthetic twin, the inclusion of clinopyroxene, overgrowth in olivine, and sieved texture in plagioclase which is the effect of alteration. This sequence can be explained as the enclosed mineral grain olivine is assumed to be the first to crystalize followed by clinopyroxene, plagioclase, K-feldspar (sanidine), quartz, and, nepheline which support /complementary with fractional crystallization trend in geochemical variation plots as discussed below. Generally the trend which show decrease in mafic mineral and increasing of felsic mineral from flood basalt to shield volcano show the decrease of magma influx (Krans et al., 2018).Basaltic rock fractional crystallization can be accessed through the plot of SiO_2 versus major oxides (Winter, 2001; Cox, 1979). With increasing SiO_2 content MgO, Fe_2O_3, CaO, TiO_2 and P_2O_5display negative trend implying fractionation of Mg- Fe- Ca- Ti and P-bearing minerals such as olivine and/or clinopyroxene, plagioclase, Fe-Ti oxides, and apatite respectively. Al_2O_3 positively correlated from basalt to trachydacite, which suggest the accumulation of plagioclase, and in rhyolite, suite shows a negative correlation with SiO_2 which implicates the fractionation of Al-bearing mineral of plagioclase. K_2O is a positive trend with increasing SiO_2, this testifies the accumulation of alkali feldspar (sanidine is common phenocryst in rhyolite).Na_2O show a positive correlation ~70% of SiO_2 and negative correlation after trachydacite which suggest the fractionation of Na-feldspar fractionation. The model of fractional crystallization for some compatible (Ni and Cr) and incompatible elements (Fig.11) of calculated trends show sharp decrease in Ni and Cr is slight as compared with Ni; whereas incompatible elements and slightly increasing up to %F = 0.4 and sharply increase up to %F = 0.

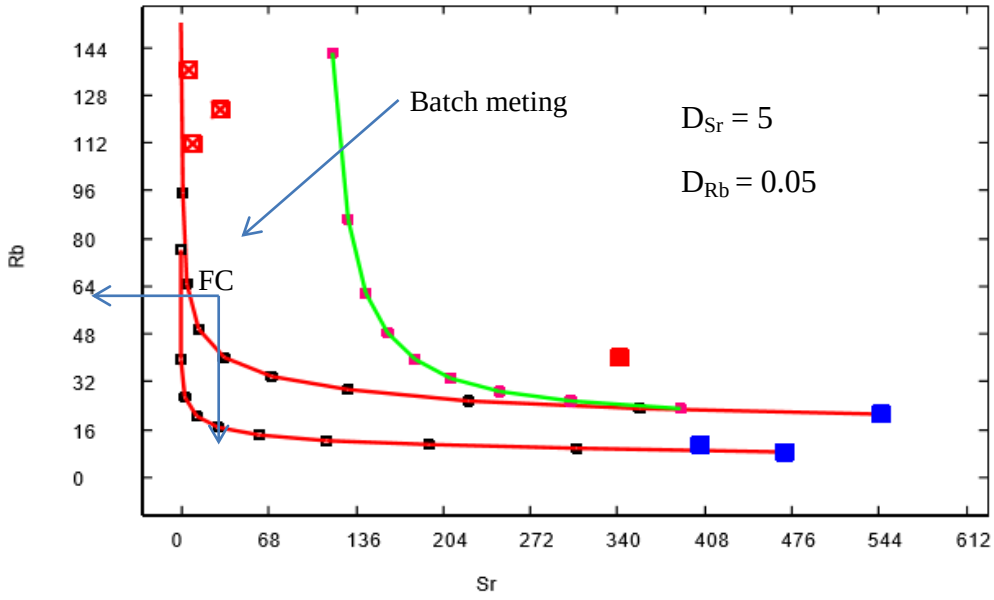

Figure 10. Variation diagram of fractional crystallization (FC) and batch melting model of compatible (Sr) vs. incompatible (Rb) trace element for lake Hayk volcanic rocks. Basalt T1S1which is less evolved rock (SiO_2 = 45.5) has been assumed as the starting composition for both fractional crystallization and batch melting. The partition coefficient for the model is 5 = Sr and 0.05= Rb (after Ewart and Griffin, 1994). Symbols the same as in (Fig.6.).

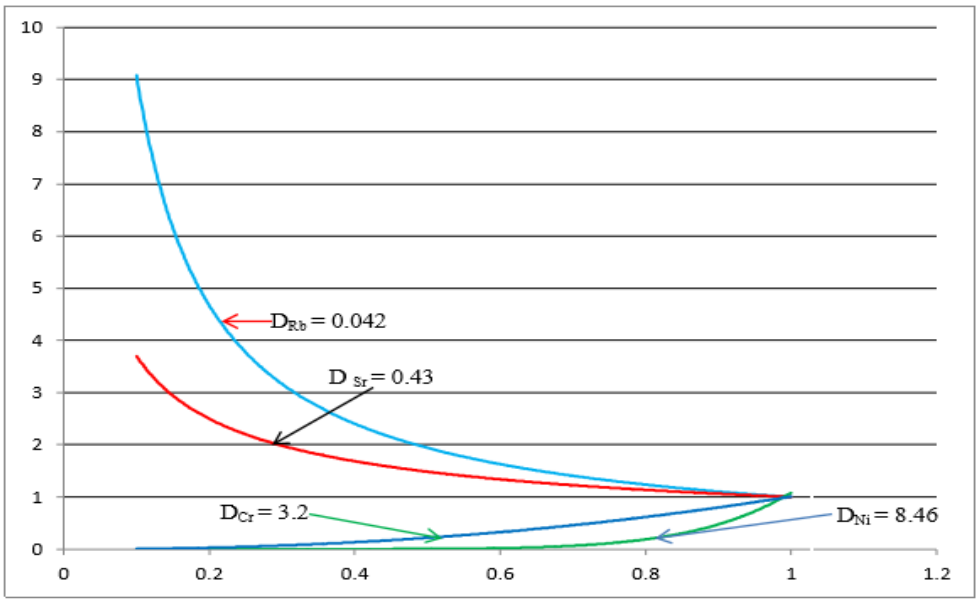

Figure 11. Fractional crystallization model for the most primitive basaltic (T1S1) rock of Lake Hayk. The weight fraction of residual liquid F%.

Table 2. Major element calculated mass balance.

	From T2S3	To T7S1	Chemical compositions Olivine	clinopyroxene	Plagioclase	Opa	%Solid Fract.	R
SiO2	48.4	55.9	40.66	47.15	50.71	0		0.003
TiO2	2.08	1.96	0	3.38	0	24.91		0.397
Al2O3	15.25	15.15	0	4.78	30.67	1.46		0.037
FeOtot	10.71	10	23.44	10.99	0.54	71.73	**60.51**	-0.156
MnO	0.18	0.17	0.35	0.19	0	0.64		-0.027
MgO	6.16	3.94	34.88	11.86	0.18	1.24		0.069
CaO	11.75	7.61	0.76	21.09	14.72	0		-0.082
Na2O	2.66	3.34	0	0.54	3.05	0		-0.412
K2O	0.45	1.88	0	0	0.14	0.01		0.34
P2O5	0.28	0.29	---	---	---	---		-0.169
Fract. Solid wt.%			**-42.5**	**-32.25**	**-21.74**	**-3.48**	**∑R² =**	**0.51**
	From T7S1	To T3S6	Olivine	Clinopyroxene	Alkali Feldspar	Opaque	%Solid Fract.	R
SiO_2	55.9	66.7	39.87	49.06	51.92	0.51		-0.093
TiO_2	1.96	1.08	0.03	0	0.77	50.02		-0.311
Al_2O_3	15.15	13	0	32.14	1.85	0		0.547
FeOtot	10	4.83	14.06	0.27	32.19	46.37	**43.41**	0.025
MnO	0.17	0.24	0.22	0	0	1.44		-0.014
MgO	3.94	0.92	45.38	0.2	0	0.46		0.271
CaO	7.61	1	0.25	15.38	0	0.71		-0.583
Na_2O	3.34	4.69	0.04	2.57	12.86	0		0.58
K_2O	1.88	4.48	0.01	0.17	0.19	0		0.27
P_2O_5	0.29	0.26	---	---	---	---		-0.169
Fract. Solid wt.%			**-14.61**	**-57.99**	**-19.67**	**-7.72**	**∑R² =**	**1.3**
	From T3S6	To T3S4	Olivine	Clinopyroxene	Sanidine	Opaque	%Solid Fract.	R
SiO_2	66.7	71.3	29.84	48.46	68.31	0		0.26
TiO_2	1.08	0.54	0	0.46	0	22.57		-0.15
Al_2O_3	13	11.95	0	0.2	18.74	0.28		-0.24
FeOtot	4.83	3.1	64.69	28.6	0.38	74.56		0.312
MnO	0.24	0.08	4.73	1.7	0	2.44	**29.47**	-0.115
MgO	0.92	0.25	0.43	1.77	0	0.12		0.017
CaO	1	0.28	0.31	18.4	0.07	0		-0.203
Na_2O	4.69	4.4	0	1.42	9.17	0		0.651
K_2O	4.48	5.02	0	0	3.33	0.01		-0.325
P_2O_5	0.26	0.09	---	---	---	---		-0.207
Fract. Solid wt.%			**-5.89**	**-9.6**	**-77.74**	**-6.77**	**∑R² =**	**0.872**

In order to test fractional crystallization hypothesis major elements mass balance calculated (Table 2). Major element modeled based on the calculation of mass balance by following steps from the most mafic to felsic rocks (Stormer and Nicholls, 1978). The mineral chemistry of basaltic rock is taken from northwestern Ethiopia flood basalt (Pik et al.,1998) and basaltic andesite to rhyolite rock is from Boseti volcanic complex of main Ethiopian rift(Ronga et al., 2009), this choice is due to minerals of rift margin mineral chemistry is not available. The calculated mass balance indicates that the evolution modeled from basalt (T2S3) to basaltic andesite (T7S1) by 60.51% solid fractional crystallization with sum of the calculated residual (R2) of 0.51.The evolutions from basaltic andesite (T2S3) to trachydacite (T3S6) by 43.41% of solid fractional crystallization with sum of the calculated residual (R2) of 1.3 and trachydacite (T3S6) to rhyolite (T5S2) by 29.47% of solid fractional crystallization with sum of the calculated residual (R2) of 0.8721. The variation diagram of major element against silica of the calculated composition and the analyzed/parent composition fit linear to curvilinear line which suggest the fractional crystallization is the major process.

Crustal contamination

The studied samples of lake Hayk basalts, have a positive anomaly of Nb and Ta (with exception of a slight trough in a sample (T7S5 slight trough at Ta)) and trachydacite to rhyolite show slight trough at Nd and positive spike at Ta on the primitive mantle normalized multi-element variation diagrams (McDonough and Sun, 1989) as illustrated in the previous section (fig.10B), and this testifies there is minimal crustal contamination in basalt (with exception of T7S5) than trachydacite to rhyolite (Rollinson., 1993). Basaltic andesite (T7S1) show a negative anomaly of Nb and Ta with high Rb and Th which suggest that the involvement of upper crust or contaminated by upper curst (Dereje Ayalew et al., 2019). Basalt have low Rb/Nb = 0.5 - 0.58, La/Nb = 0.88 - 1.06 and higher TiO_2 = 2.08 - 3.04, basaltic andecite

have higher Rb/Nb =2.7, La/Nb = 1.81 and low TiO_2 1.96 and rhyolite Rb/Nb = 0.97-1.69, La/Nb = 0.51 - 1.08 and lower TiO_2 = 0.41 - 0.71this suggest that there is more crustal involvement in basaltic andecite as compared to basalt and rhyolite; whereas lower in basalt as relative to rhyolite(Rollinson, 1993; Dereje Ayalew and Gezahegne Yirgu, 2003). Further, MgO against incompatible trace elements such as Th, La, and U have a negative correlation as shown below (Fig.12), this testifies that there is insignificant continental crust involvement (Zhang et al., 2009). Furthermore, Ce/Pb has a positive correlation with MgO (fig.12B), this suggest that crustal contamination is minimal towards basaltic rock which have maximum concentration MgO and Ce/Pb, whereas felsic rocks are contaminated (Dereje Ayalew et al., 2016; Haldera et al., 2020).

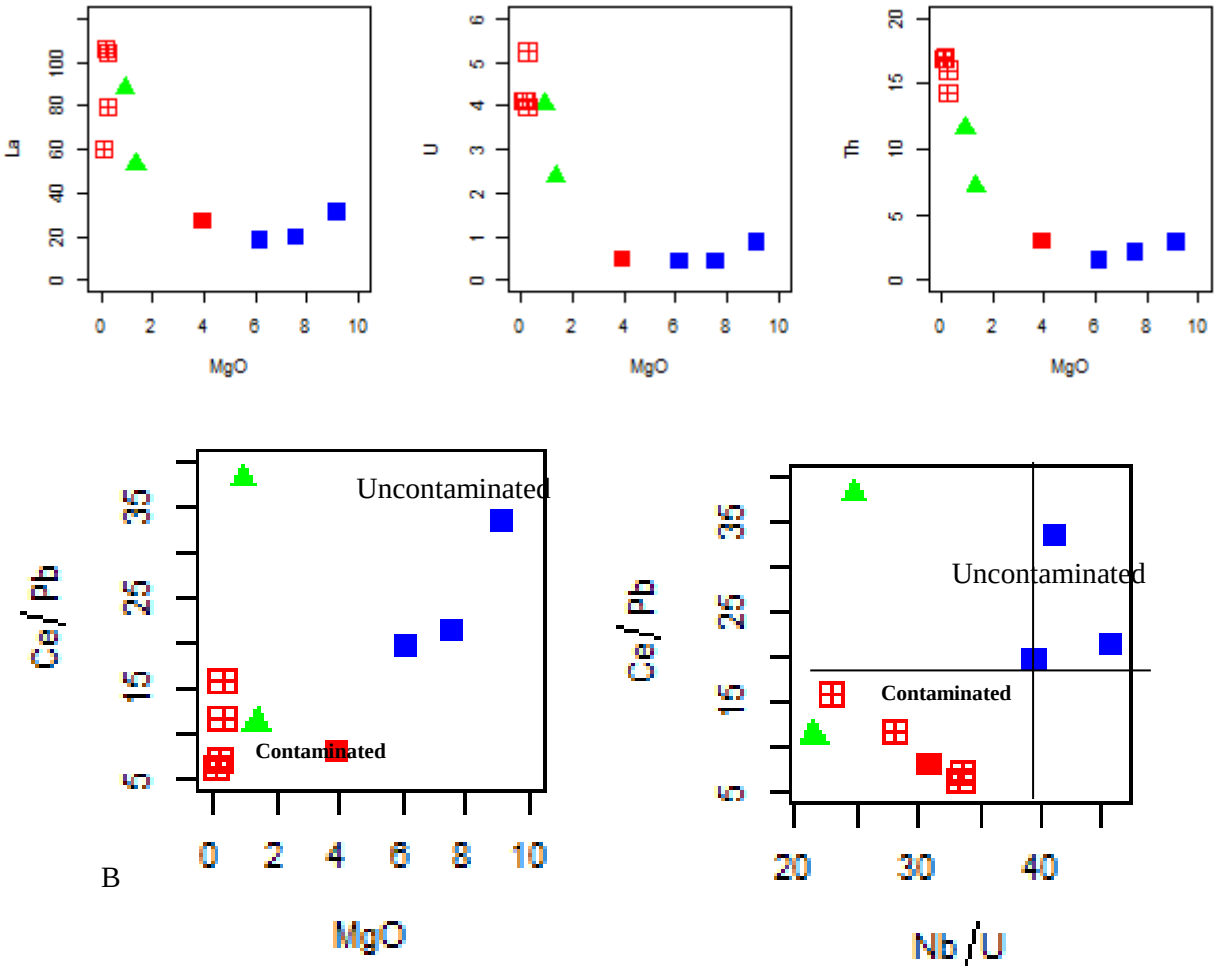

Figure 12. MgO against for selected incompatible trace elements (La, U, Th) diagrams of the Lake Hayk volcanic rocks. Symbols same as in fig.6.

Magma generation and source rock characterization

The basalt rock unit from lake Hayk is characterized by low CaO/Al_2O_3 ratios (0.71–0.95) and in primitive mantle normalized multi-element variation diagram (Sun and McDonough, 1989) HREE relatively no fractionation/flat patterns with (TbN/YbN = 1.75-2.33)(fig.9c and). This value most likely suggests a mantle source containing spinel rather than garnet and the slight fractionation of HREE show the sight effect of garnet (Dereje Ayalew et al., 2016). Further, the basalts in the studied area have positive anomaly of Ba and a negative anomaly of K (positive anomaly at (T7S5)) in comparison to other primitive mantle normalized multi-element variation diagrams (Fig.9 C). Such positive and negative anomaly of Ba and K respectively, testify related to amphibole and phlogopite(for K positive sample(T7S5) in the mantle source (e.g., Jung et al., 2005, 2012; Furman and Graham, 1999; Dereje Ayalew et al., 2006; Rooney et al., 2014). Additionally, basalt samples have Na_2O > K_2O, such observation suggests that the source is formed through melting of the amphibole-bearing mantle (Rosenthal et al., 2009).Based on the above

observation the lake Hayk basalts were derived from the melting of amphibole-bearing spinel peridotite sources rather than Phlogopite bearing source (Dereje Ayalew et al., 2016). Amphibole may also occur in the lithospheric mantle, because it is not stable in the sub-lithospheric mantle source of asthenosphere or mantle plume (Class and Goldstein, 1997).

Petrogenesis of rhyolites

To explain the petrogenesis of rhyolitic lava and associated rhyolitic tuff, rhyolitic ignimbrite, glassy rhyolite, and pumice (60-81 wt% SiO_2), several petrogenetic models describing the origin of silicic volcanic rocks in mafic LIPs have been proposed. These include: (i) fractional crystallization of parental mafic magmas (e.g., Ayalew et al., 2002; Mahoney et al., 2008; Melluso et al., 2008; Natali et al., 2011; Cucciniello et al., 2019) (ii) re-melting of underplated basaltic intrusions (Cleverly et al., 1984; Harris and Erlank, 1992; Miller and Harris, 2007), (iii) assimilation of crustal material by parental mafic magmas and simultaneous fractional crystallization (AFC) (Chazot and Bertrand, 1993; Baker et al., 2000; Melluso et al., 2001; Dereje Ayalew and Gezahegne Yirgu, 2003; Peccerillo et al., 2003; Mahoney et al., 2008; Sheth and Melluso, 2008; Cucciniello et al., 2011), and (iv) melting of continental crust (Tian et al., 2010; Shellnutt et al., 2012; Huang et al., 2015). Significant fractional crystallization produces rhyolites with steep negative slopes in bivariate major oxides plots and a modest to no Nb-Ta anomaly (Haldera et al., 2020), whereas strong crustal input produces rhyolites with significant Nb-Ta negative anomalies. Hence, the rhyolites of Lake Hayk have steep negative correlation in bivariate major oxides such as MgO, Fe_2O_3, TiO, and CaO against SiO_2, as well as a positive anomaly of Ta with a slight Nb trough, implying that rhyolites formed by fractional crystallization of mafic magma with insignificant crustal contribution. Further, rhyolites formed by crustal melting have an Rb/Nb ratio >10; whereas, the analyzed rhyolitic samples Rb/Nb < 1.69 this indicates that partial melting of the continental crust did not contribute to the formation of rhyolites ((fig.14b). Plot of TiO_2 vs. SiO_2 (Fig.7) for volcanic rock of lake Hayk shows negative correlations and a positive correlation of HFSE such as Zr vs. Rb, Zr vs. Hf, Zr vs. Nb, and Zr vs. Ta forming a single trend that show the genetic relationship or co-magmatic nature of the basaltic and rhyolitic rocks around Lake Hayk area (Haldera et al., 2020). This suggests that rhyolites are related to the basalts by Fractional crystallization as illustrated in (fig.10). The Zr/Nb ratio of basalt to rhyolite vary between 7.01-8.76 and basaltic andesite (T7S1) and one rhyolite (T1S2 EA) sample Zr/Nb = 14.43 and 10.17 respectively. The little variation of Zr/Nb ratios in basalt to rhyolites indicates that fractional crystallization has been the major process in their history of petrogenesis (Barberi et al., 1975). The only exceptions are basaltic andesite and one rhyolite sample, which have a different array (high Zr/Nb of T2S1 EA = 10.17 and T7S1 - 14.43), suggesting derivation from a depleted plume head source (Ferguson et al.,2010).

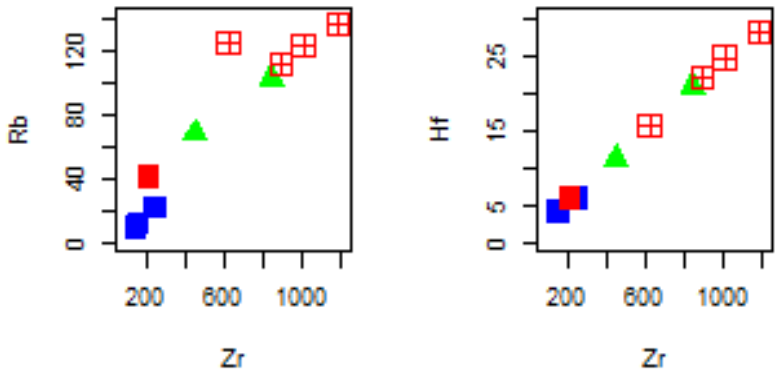

Figure 13. Incompatible against incompatible trace elements variation diagrams (ppm)of Lake Hayk, analyzed samples. Symbols the same as in(Fig.6).

Rhyolites that have (Gd/Lu)N ratio (>2.2), suggest that the parental melts may have been generated at higher depths in the garnet stability field (Haldera et al., 2020).The ratio of (Gd/Lu)N of rhyolite in the study area varies between 1.59 - 2.48. Hence the rhyolite sample (T3S4 GdN/LuN = 2.24 and T1S1 EA GdN/LuN = 2.48) from Lake Hayk which has (Gd/Lu)N ratio (>2.2) implicate that parental melts may have been generated at higher depths in the garnet stability field and the other two sample(T5S2 Gd/Lu)N = 1.72 and T1S3 GdN/LuN =1.59) which have (Gd/Lu)N ratio (<2.2) are from spinel stability field. The Rb against Sr bivariate plot of rhyolite (Fig .14 A), shows a large variation in Sr (8.6 – 151ppm) with limited variation in Rb (111.5 – 136ppm) abundances. Accordingly, such highly incompatible against highly compatible trace element trend suggests that the rhyolite of the Lake Hayk area related to erupted basaltic magmas by the fractional crystallization process than partial melting (Dereje Ayalew et al., 2019; Haldera et al.,2020).

Eventually, the stratigraphy and petrography which supports the above interpretation because stratigraphically basaltic rock units are unconformably overlain by rhyolitic rock unit of different age separated by paleosol, and petrographically from bottom to top are as follow; olivine, clinopyroxene, plagioclase, (very low), k-feldspar (sanidine) and quartz which show they originated within the same magma chamber and that the rhyolitic volcanic rocks were derived by fractional crystallization of the mafic/basaltic magma.

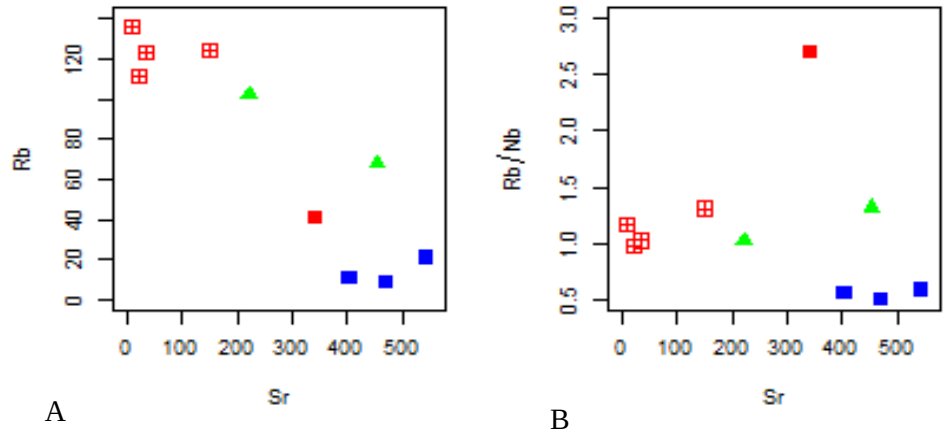

Figure 14. Variation diagrams of (A), Sr vs. Rb and (B),Sr vs. Rb/Nb of Lake Hayk area volcanic rocks. Symbol the same as (fig. 6).

Comparison of lake hayk primary data with previous works

The Lake Hayk area has a bimodal composition whith scarce intermidate rock unit. As a comparison, four samples (two basalt, one rhyiolite, and one trachyite) from the Guguftu shield volcanics (Kiffer et al., 2004) and eleven samples from Wegel Tena, Kobo, and Hara (Ayalew et al., 2019). The outcomes of the samples are generally consistent with the primary data studied in the current study approach. Ten samples from Lake Hayk and fifteen samples from previous samples were combined for comparison in various diagrams. Both major and trace Variation Elements diagrams of the investigated primary basalts of Lake Hayk plotted against previous basalts and primary felsic sample plotted against previous felsic sample demonstrate that the signatures are most likely the same. When compared to previously reported Gugugufttu shield and marginal Hara,kobo and Wegel Tena volcanic suites of geochemical data obtained by previous investigations, the current study does not demonstrate a significant difference in composition. With the exception one basalt from Guguftu, almost all samples from Lake Hayk fall near the transition between alkaline and sub alkaline fields. As shown in (fg.15) below, the other basalt, trachyte, and rhyolite samples are alkaline, as well as one trachydacite, basaltic trachyte, and rhyolite sample from Lake Hayk, Hara, and Kobo.

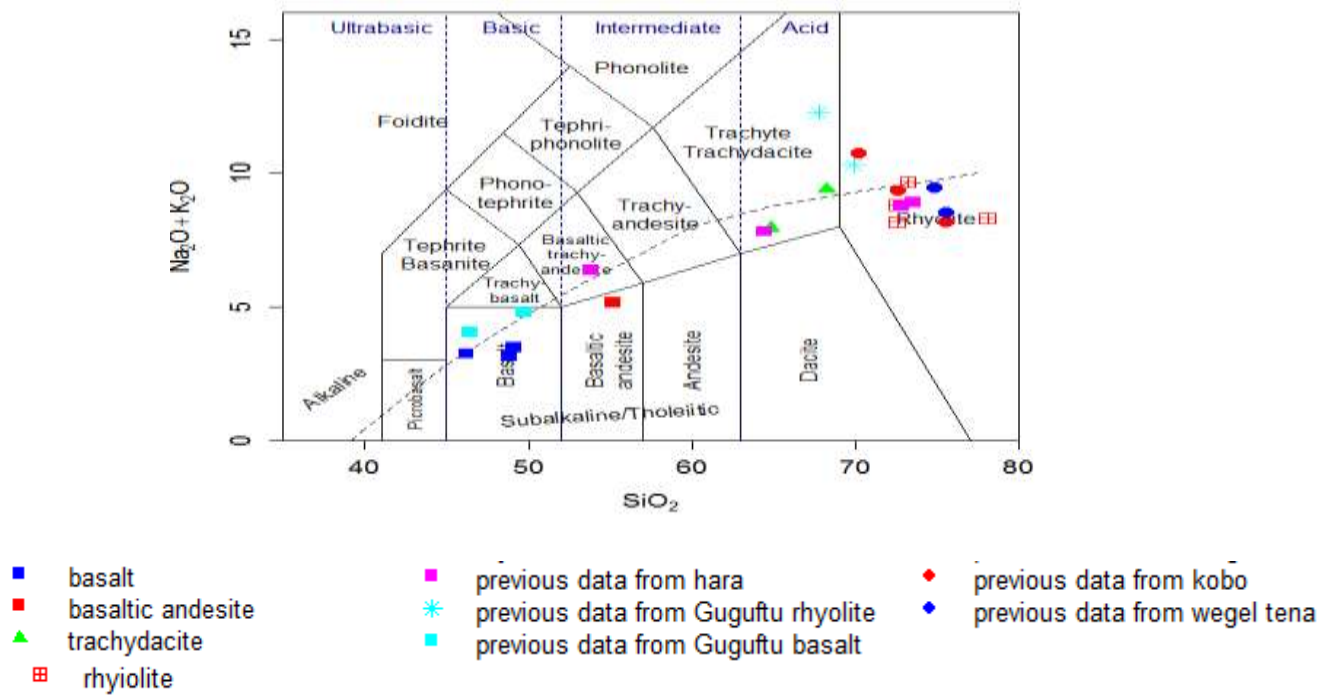

Figure 15. TAS classification diagrams of Lake Hayk flood basalts and rhyolite for composition of Lake Hayk basalt to rhyolite from the previous works.

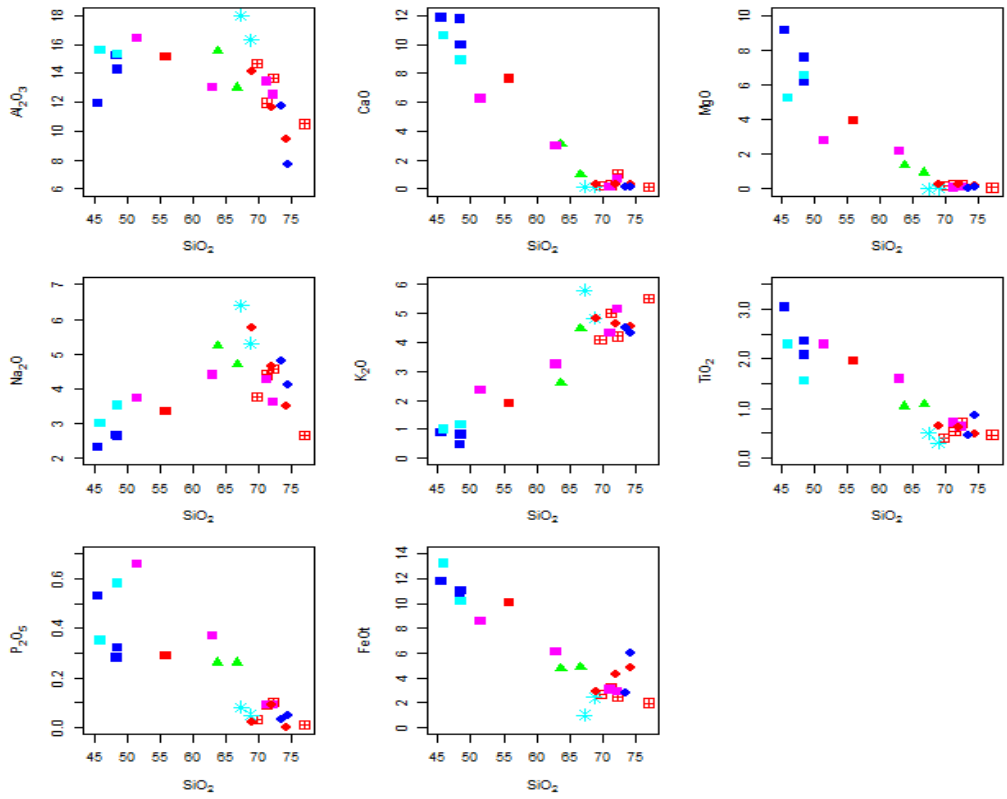

Figure 16. Variation diagrams of major element contents as a function of SiO_2 for comparison of Lake Hayk volcanic rock with previous work. Symbol the same as (fig .15).

The variation diagram of major element against SiO_2 (fig.16) for both primary and previous data show the same trend (primary basalt with previous basalt, primary basaltic andesite with previous basaltic andecite and primary felsic with previous felsic). Both primary and previous samples show steep negative trend of these compatible trace elements and the accommodating major elements (Fe, Mg, Ca); show pronounced evolution trend starting from basalt-intermediate rhyolite suites. The available primary data show Lake Hayk rhyolites show similar signature of major and trace element abundance with Hara, kobo, and Wegel Tena silicics analyzed in previous works. Basaltic systems show Sr depletion in response to the fractionation of plagioclase and or crustal assimilation (Haliday et al, 1991); and Rb increases corresponding to the more or less vertical trend (see Fig. 6.10). Incompatible trace elements like Sr drops to very low concentrations both in Hara, Guguftu and Lake Hayk felsic rocks; whereas strongly incompatible trace elements like Rb, Nb, and La showing very high concentration. Previous work results have presented that, the felsic rocks of Hara formation display similar patterns with Lake Hayk felsic rock.

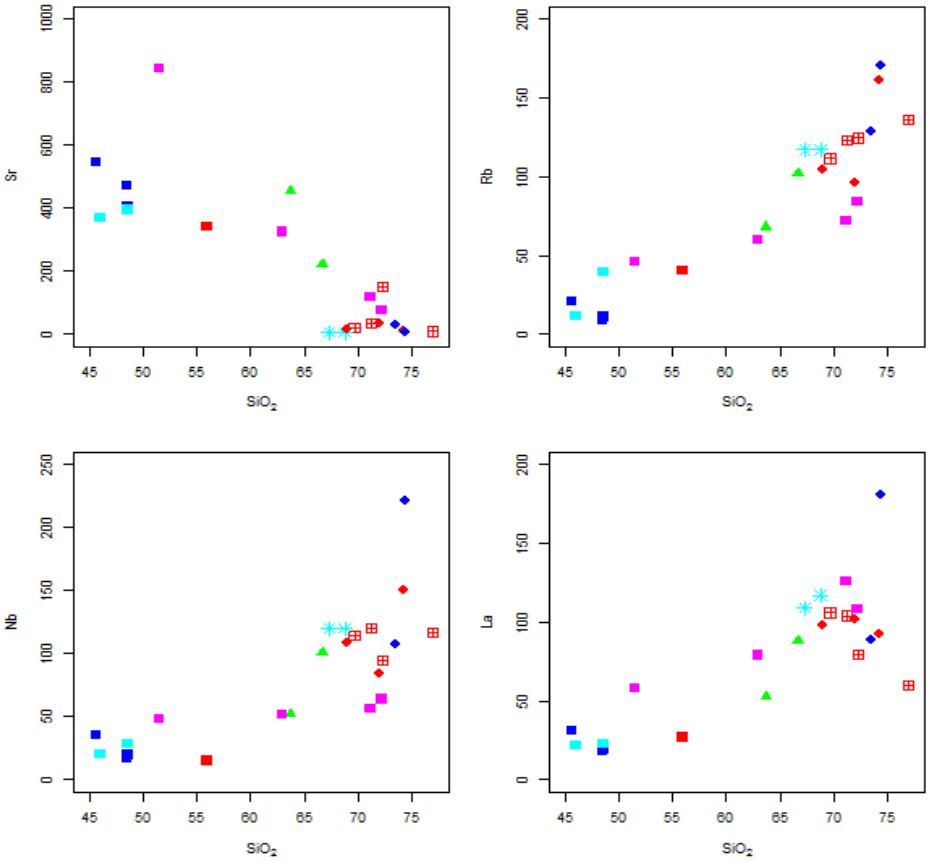

Figure 17.Trace element variation diagrams show the variation of incompatible trace elements against SiO_2 for composition of Lake Hayk basalt to rhyolite to the previous work.. Symbols are the same as in Fig.15.

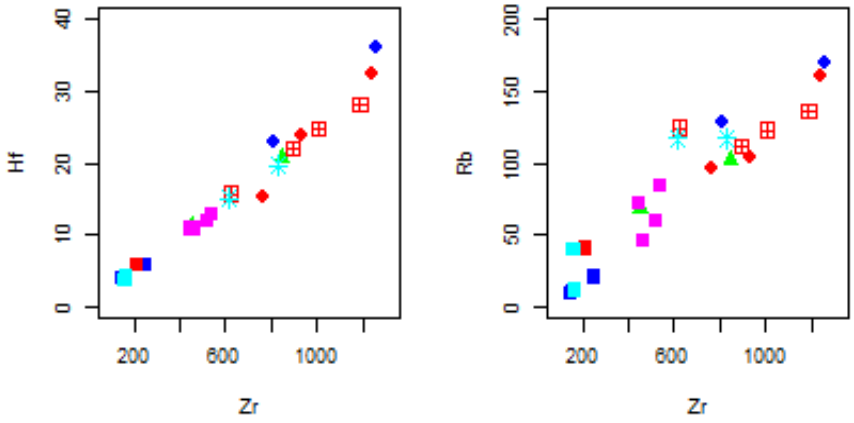

Figure 18. plots of Rb against Zr variation diagram which shows comparison of Lake Hayk volcanic rock with previous work. Symbol the same as fig .15.

Volcanic rock of lake Hayk, Wegel Tena, Guguftu and Hara plots of TiO_2 vs. SiO_2 (Fig.16) shows negative correlations and a positive correlation of HFSE such as Zr vs. Rb, Zr vs. Hf, Zr vs. Nb, and Zr vs. Ta forming a single trend that show the genetic relationship or co-magmatic nature of the basaltic and rhyolitic rocks those area.

Table 3. 1: Trace element and TiO_2 of the Lake Hayk area volcanic rocks compared with other marginal rhyolites and Guguftu shield volcano.

	Rock type based on TSA classification	Rb/Nb	La/Nb	TiO_2	Source of data
Hara	Basaltic trachyte	0.96	1.21	2.29	Ayalew et al.,(2019)
	Trachydacite	1.16	1.52	1.60	
	Rhyolite	1.13-1.19	1.49-2.25	0.57 – 071	
Guguftu	Basalt	0.57-1.41	0.81-1.07	1.56 – 2.29	
	Trachydacite	0.98	0.91	0.51	Kieffer et al.,(2004)
	Rhyolite	0.98	0.98	0.53	
Kobo	Rhyolite	0.95 – 1.14	0.91-1.21	0.63 -0.65	Ayalew et al.,(2019)
Wegel Tena	Rhyolite	0.77-1.21	0.81- 0.83	0.46 – 0.86	Ayalew and Yirgu,(2003)
Lake Hayk	Basalt	0.5-0.58	0.88-1.06	2.08-3.04	present study of this work
	Basaltic andesite	2.70	1.18	1.96	
	Trachydacite	1.01-1.32	0.88-1.02	1.04-1.08	
	Rhyolite	0.97-1.69	0.51-1.08	0.41-0.71	

Furthermore, Lake Hayk rhyolites unit have the same Rb/Nb (0.51-1.08) and La/Nb (0.41-0.71) ratios to that of Kobo, Wegel Tena, and Guguftu rhyolite rock units; whereas relatively lower than Hara rhyolite rock unit, which implicate that in Kobo, Guguftu, and Lake Hayk rhyolites unit there is only limited crustal material was involved in their genesis or minimal amount of crustal contamination than Hara rhyolite. Generally this work supports the previous work.

CONCLUSIONS

The following conclusions have been drawn based on the, field observations, petrographic and geochemical data obtained in this study:

➢ Major and trace element geochemistry data testify that volcanic rocks of Lake Hayk are a bimodal suite, with scarce intermediate composition. The Oligocene basalts and rhyolite rocks are transitional to tholeiitic/sub alkaline

affinity and rhyolite rocks are peraluminous (exceptionally one rhyolite rock sample (T3S4) is peralkaline).

- There is minimal to no crustal contamination in basalt (with exception of T7S5) relatively to trachydacite to rhyolite.
- Basaltic andesite shows evidence of involvement of upper crust or contaminated by upper crust.
- The source for volcanic rock from lake Hayk area is the amphibole-bearing mantle. Parental melts for two rhyolites may have been generated at higher depths in the garnet stability field and for two other samples (T5S2 and T1S3 from spinel stability field.
- The parallel pattern of basalt and rhyolite in chondrite normalized REE pattern, Nb, Hf, Ta, and Rb against Zr, and flood basalt and rhyolitic flow range in age from 28.5 to 31 Ma do to these evidences basaltic to rhyolitic rocks generated from the same magma source/ co-magmatic nature.
- The rhyolitic rock units of Lake Hayk area are formed by fractional crystallization of mafic parental magma rather than assimilation of continental crust.
- Comparison of geochemical content Lake Hayk bimodal volcanic rock with the plateau formations shows that basalts have a similar geochemical pattern with HT1 type continental flood basalt whereas the trace element ratios of the Lake Hayk area rhyolites agree with Kobo, Guguftu, and Lake Hayk rhyolites unit.

ACKNOWLEDGMENTS

Firstly, the authors would like to extend grateful to Samara University Geology Department and Addis Ababa University, School of Earth Science for its complete support from the beginning to the end of this research work. Author's gratitude also goes to vice president for research and technology transfer (VPRTT) for funding the research fully.

REFERENCE

1. Abbate , E., Sagri, M. (1980).Volcanites of Ethiopian and Somali Plateaus and major tectonic lines. Atti Convegni Acc Lincei Roma 47:219– 227
2. Barberi F., Ferrara G., Santacroce R., Treuil M., and Varet J. (1975). A transitional basalt-pantellerite sequence of fractional crystallization, the Boina Centre (Afar Rift, Ethiopia). J. Petrol. 16, 22–56.
3. Blanford, W.T. (1870).Observations on the geology and zoology of Abyssinia. Made during the progress of the British Expedition to that country in1867-8. Macmillan. 487p.
4. Class, C., Goldstein, S. (1997). Plume lithosphere interaction in the ocean basins: constraints from source mineralogy. Earth and Planetary Science Letters 150, 245–260.
5. Courtillot, V., Jaupart, C., Manighetti, I., Tapponnier, P. and Besse, J. (1999).On causal links between flood basalts and continental breakup. Earth and Planetary Science Letters, 166: 177-195.
6. Coulie, E. (2001).Chronologie Ar/Ar et K/Ar de la dislocation du plateou ethiopien et de la dechirure continetale dans la Corne de I"Afrique depuis 30 Ma. Ph.D. thesis, University de paris Sud. Orsay.
7. Coulié, E., Quidelleur, X., Gillot ,P., Courtillot ,V., Lefèvre ,J., and Chiesa, S. (2003). Comparative K-Ar and Ar/Ar dating of Ethiopian and Yemenite Oligocene volcanism: Implications for timing and duration of the Ethiopian Traps. Earth and planetary Science Letters 206, 477–492.
8. Cox, K.G., J.D. Bell and R.J. Pankhurst . (1979). The Interpretation of Igneous Rocks. Allen and Unwin.
9. Dereje Ayalew., Gezahegne Yirgu., &Pik, R. (1999). Geochemical and isotopic (Sr, Nd and Pb) characteristics of volcanic rocks from southwestern Ethiopia. *Journal of African Earth Sciences,* **29(2):** 381–391.
10. Dereje Ayalew, Barbery, P., Marty, B., Reisberg, L., Gezahegn Yirgu, and Pik, R. (2002). Source, genesis and timing of giant ignimbrite deposits associated with Ethiopian continental flood basalts. *Geochemica et Cosmochimica Acta* **66(8**): 1429-1448.
11. Dereje Ayalew and Gezahegn Yirgu. (2003).Crustal contribution to the genesis of Ethiopian Plateau rhyolitic ignimbrites, basalt and rhyolite geochemical provinciality. *Journal of the Geological society* **160(1):** 47-56.
12. Dereje Ayalew, Marty, B., Barbey, P., Gezahegn Yirgu and Endale Ketefo (2006). Sublithospheric source for quaternary alkaline Tepi shield, southwest Ethiopia. **40**: 47–56.

13. Dereje Ayalew, Jung, S., Romer, R.L., Kerstend, F., Pfänder, J.A., Garbe-Schönberg, D. (2016). Petrogenesis and origin of modern Ethiopian rift basalts: Constraints from isotope and trace element geochemistry. Lithos 258–259: 1–14

14. Dereje Ayalew1 , Pik,R., Bellahsen, N.,France,L.,and Gezahegn Yirgu.(2019).Differential Fractionation of Rhyolites During the Course of Crustal Extension, Western Afar (Ethiopian Rift). Geochemistry, Geophysics, Geosystems, 20. https://doi. org/10.1029/2018GC007446

15. Ewart, A. and Griffin, W. (1994). Application of proton-microprobe data to trace-element partitioning in volcanic rocks. Chemical Geology 117(1):251-284.

16. Ferguson,D.J.,Barnie,T.D.,Pyle,D.M.,oppenheimer, C., Yirgu, G., Lewi, E., Kidane, T. (2010). Recent rift-related volcanism in Afar, Ethiopia. Earth and Planetary Science Letters, 292, 409–418.

17. Frey, F., Green, D., Roy, S. (1978). Integrated models of basalt petrogenesis: a study of quartz tholeiites to olivine melilites from South Eastern Australia utilizing geochemical and experimental petrological data. *Journal of Petrology* **19**: 463–513.

18. Gezahegn Yirgu. (1997). Magma – crust interaction during emplacement of Cenozoic volcanism in Ethiopia: geochemical evidence from Sheno-Megezez area, central Ethiopia. *SINET: Ethiopia J. Sc.* **20(1):** 49-72.

19. Halder, M.,Paul,D.,Sensarma,S.(2020). Rhyolites in continental mafic Large Igneous Provinces: Petrology, geochemistry and petrogenesis. Geoscience Frontiers 12 (2021) 53–80. https://doi.org/10.1016/j.gsf.2020.06.011

20. Hess, P. (1992). Phase equilibria constraints on the origin of ocean floor basalts. *Geophysical Monograph*, **71**: 67–102.

21. Hawkesworth, C., Kelley, S., Turner, S., Le Roex, A. and Storey, B. (1999). Mantle processes during Gondwana break-up and dispersal. *Journal of African Earth Sciences*, **28**: 239-261.

22. Hofmann, C., Courtillot, V., Féraud, G., Rochette, P., Gezahegn Yirgu, Endale Ketefo, and Pik, R. (1997). Timing of the Ethiopian flood basalt event and implications for plume birth and global change: Nature, 389: 838–841.

23. Kazmin, V. (1973). Geological map of Ethiopia, scale 1:2,000,000. Geological Survey of Ethiopia, Addis Ababa

24. Kieffer, B., Arndt ,N., Lapierre, H., Bastien ,F., Bosh. D., Pecher, A., Yirgu,G., Ayalew, D., Weis, D., Jerram, DA., Keller ,F., Meugniot, C. (2004). Flood and shield basalts from Ethiopia: magmas from the African superswell. *J Petrol* **45**:793–834.

25. Mohr P. (1983). Ethiopian flood basalt province. Nature 303, 577–584.

26. Mohr, P. and Zanettin, B. (1988). The Ethiopian flood basalt province. In: Macdougall, J.D.(ed), continental flood basalts. Klwuer Academic Publishers, Dordrecht, PP 63-110.

27. Nakamura, N. (1974). Determination of REE, Ba, Fe, Mg, Na and K in carbonaceous and ordinary chondrite. Geochimica Cosmochimica Acta, 38: 757-775.

28. Peccerillo, A., Barberio, M.R., Yirgu, G., Ayalew, D., Barbieri, M., Wu,T.W. (2003). Relationships between mafic and peralkaline acid magmatism in continental rift settings: a petrological, geochemical and isotopic study of the Gedemsa volcano, central Ethiopian rift. *Journal of Petrology* **44**: 2003–2032.

29. Pik, R., Deniel, C., Coulon, C., Yirgu, G., Hoffmann, C. & Ayalew, D. (1998). The northwestern Ethiopian Plateau flood basalts: classification and spatial distribution of magma types. *Journal of Volcanology and Geothermal Research* **81**: 91-111.

30. Pik, R., Deniel, C., Coulon, C., Yirgu, G. & Marty, B. (1999). Isotopic and trace element signatures of Ethiopian basalts: evidence for plume lithospheric interactions. Geochimica et Cosmochimica Acta 63,2263-2279.

31. Richards, M.A., Duncan, R.A., Courtillot, V.E.(1989). Flood basalts and hot-spot tracks: plume heads and tails. Science 246, 103–107.

32. Rollinson, H.R. (1993). Using Geochemical Data: Evaluation, Presentation and Interpretation. Longman Group, London, 352p.

33. Ronga,F.,Lustrino,M.,Marzoli,A.,Melluso,L.(2009). Petrogenesis of a basalt-comenditepantellerite rock suite: the Boseti Volcanic Complex (Main Ethiopian Rift). Mineral. Petrol. 160, 407–425. https://doi.org/10.1007/s00410-009-0485-3.

34. Rooney, T., Furman, T., Bastow, I., Dereje Ayalew, and Gezahegn Yirgu. (2017). Lithospheric modification during crustal extension in the Main Ethiopian Rift. *Journal of Geophysical Research: Solid Earth* 1978–2012.

35. Rosenthal, A., Foley, S.F., Pearson, D.G., Nowell, B.M., Tappe, S.(2009). Petrogenesis of strongly alkaline primitive volcanic rocks at the propagating tip of the western branch of the East African Rift. Earth and Planetary Science Letters 284, 236–248.

36. Ukstins, I.A., Renne, P.R., Wolfeden, E., Baker, J., Dereje Ayalew and Menzies, M. (2002).Matching conjugate volcanic rifted margins: 40Ar/39Ar chronostratigraphy of pre- and syn-rift bimodal flood volcanism in

Ethiopia and Yemen. Earth and Planetary Science Letters, 198:289–306.

37. Winter, J.D.(2001). An introduction to Igneous and Metamorphic petrology, Prince Hall Inc., Upper Saddle River, New Jersey

38. Zhang J.J., Zheng, Y.F. and, Zi-Fu Zhao, Z.F. (2009). Geochemical evidence for interaction between oceanic crust and lithospheric mantle in the origin of Cenozoic continental basalts in east-central China. Lithos.110, 305–326